Kondo disorder: a possible route towards non-Fermi-liquid behaviour

E Miranda†§, V Dobrosavljević† and G Kotliar‡

† National High Magnetic Field Laboratory, Florida State University, 1800 E Paul Dirac Drive, Tallahassee, FL 32306, USA
‡ Serin Physics Laboratory, Rutgers University, PO Box 849, Piscataway, NJ 08855, USA

Abstract. We present a general model of disorder in Kondo alloys that, under certain conditions, leads to non-Fermi-liquid behaviour. The central underlying idea is the presence of a distribution of local Kondo temperature scales. If this distribution is broad enough, such that there are sites with arbitrarily low Kondo temperatures, a non-Fermi-liquid phase is formed. We analyse thermodynamics and transport in this approach and show it is consistent with a number of Kondo alloys. We also compare the predictions of this model with the measured dynamical magnetic response of these systems.

1. Introduction

Since its introduction by Landau in 1956, the Fermi-liquid paradigm has been the most robust stepping-stone of the theory of metals [1]. Its central assumption is the existence of a one-to-one correspondence between the excitations of a free Fermi gas and an interacting fermionic system. Even though originally formulated to explain the behaviour of a neutral Fermi system (^{3}He), it has formed the basis of much of our understanding of what goes on in metallic systems. It lies behind such successful theories as Migdal's electron–phonon theory and provides the background upon which instabilities such as superconductivity can be understood. It has proved to be a valuable guide in the analysis of even very strongly correlated systems, such as some of the heavy-fermion metals, where the theory seems to survive the most extreme circumstances, with enormous renormalizations in the quasiparticle effective mass.

The very idea of a correspondence between the low-lying excitations of an interacting system and those of a reference one has proved more general than the original strict application envisioned by Landau. Indeed, this principle of 'adiabatic continuity' [2] can be found in very diverse situations with very different and sometimes non-trivial reference systems. For example, in the so-called Fermi-liquid theory of the Kondo or Anderson impurity problem, the reference system is a non-interacting scattering centre embedded in a free Fermi sea [3, 4]. Other examples include superfluid ^{3}He [5], atomic nuclei [6] and interacting disordered metals [7]. The corresponding reference systems, in these latter cases, are the BCS model of pairing, a shell model of the nucleus and a model of diffusive electrons in a random potential, respectively.

§ To whom any correspondence should be addressed.

Given this operational definition of a Fermi liquid, the question of whether a particular system behaves as a Fermi liquid or not can be a rather delicate one. It is necessary first to determine what is a natural reference system for a particular compound and then find out whether the compound can fit a description which is adiabatically connected to the reference one. We cannot overemphasize the fact that this is not always a straightforward task. Daunting as the task may be, researchers have nonetheless developed rules of thumb to classify various systems as non-Fermi liquids. One such commonly used criterion is a resistivity which depends linearly on the temperature at low temperatures, a result certainly inconsistent with a clean Fermi liquid. However, helpful as these empirical tests are, as a matter of scientific rigour, we must stress that the classification of a certain system as a non-Fermi liquid often involves careful cross-checking between experiment and theory. This is particularly critical when the system is disordered. With these caveats in mind, we can proceed to consider the question of non-Fermi-liquid behaviour.

In recent years, a growing number of metallic compounds have come to be known as counter-examples to the old Fermi-liquid paradigm. This is usually taken to mean that the adiabatic continuity hypothesis appears to break down, *if one assumes the most natural reference system for the system under study.* This has been perhaps most strongly emphasized in the case of the high-T_c cuprate superconductors [8], where Landau's original Fermi-liquid theory is unexpectedly violated in the normal state. In addition, some heavy-fermion systems have also been discovered which do not seem to fit the general picture of a Fermi liquid [9, 10]. The bulk of this evidence has in effect turned the study of non-Fermi-liquid behaviour into an independent frontier area of research whose ramifications can only be dimly glimpsed. The main goal is to determine *the possible routes* towards the breakdown of Fermi-liquid theory and to classify what new low-lying excitations are present in these systems.

Among the non-Fermi-liquid candidates, some should be classified as belonging to the heavy-fermion family. This is taken to mean, in this context, that for some range of composition or for certain values of external parameters—such as pressure or magnetic field—these compounds show typical heavy-fermion physics with high-temperature incoherent Kondo behaviour accompanied by the formation of a low-temperature heavy Fermi liquid, with or without magnetic or superconducting order [11]. However, for the more interesting values of these parameters, their behaviour is not that of a Fermi liquid.

Some of the heavy-fermion non-Fermi-liquid metals have been convincingly associated with the proximity to a quantum critical point. These are the alloy $CeCu_{6-x}Au_x$ [12] and the compound $CePd_2Si_2$ [13]. Both systems show antiferromagnetism: $CeCu_{6-x}Au_x$ for $x > 0.1$ and $CePd_2Si_2$ for pressures $P < 26$ kbar. At the critical values of these parameters, the Néel temperature T_N vanishes and the behaviour of the system appears to be governed by the zero-temperature critical point. The anomalous non-Fermi-liquid behaviour of these compounds is exemplified by the resistivity which is given by $\rho \approx \rho_0 + AT$ in $CeCu_{5.9}Au_{0.1}$ and as $\rho \approx \rho_0 + BT^{1.2}$ in $CePd_2Si_2$ at $P = 26$ kbar. In the latter case, the non-Fermi-liquid behaviour is interrupted by what appears to be a phase transition into a superconducting state at $T_c \approx 0.4$ K. The thermodynamic response of $CeCu_{5.9}Au_{0.1}$ is also anomalous with the specific heat $C/T \approx a \ln(T/T_0)$ and $\chi \approx \chi_0(1 - \alpha\sqrt{T})$. In addition, external pressure can suppress T_N to zero in $CeCu_{5.7}Au_{0.3}$ and the anomalous behaviour associated with the quantum critical point can be recovered. Though the non-Fermi-liquid behaviour can be reasonably ascribed to the proximity of a quantum critical point, a complete theory does not yet seem to exist [14].

In contrast to the latter compounds, a series of other alloys also seems to show

characteristic non-Fermi-liquid behaviour which cannot be clearly associated with quantum criticality. A partial list of these is given in table 1, together with their corresponding resistivity, specific heat and magnetic susceptibility (see also references [9, 10]). All of them show anomalous thermodynamic and transport properties incompatible with a Fermi-liquid description.

Table 1. Heavy-fermion alloys which exhibit non-Fermi-liquid behaviour not obviously ascribed to the proximity to a quantum critical point and their properties. Here, $\rho(T)$ is the DC resistivity, $C(T)$ is the specific heat, $\chi(T)$ is the magnetic susceptibility and $1/\tau(\omega)$ is the frequency-dependent scattering rate. Below, $A > 0$ and $\omega_0 > 0$.

Compounds	$\rho(T)$	$C(T)/T$	$\chi(T)$	$1/\tau(\omega)(T = 0)$
$UCu_{5-x}Pd_x$ [15, 16]	$\rho_0 - AT$	$a \ln(T_0/T)$	$a \ln(T_0/T)$	$(1/\tau_0)(1 - \omega/\omega_0)$
$M_{1-x}U_xPd_3$ (M = Sc, Y) [17, 18]	$\rho_0 - AT$	$a \ln(T_0/T)$	$AT^{-0.3}$	$(1/\tau_0)(1 - \omega/\omega_0)$
$La_{1-x}Ce_xCu_{2.2}Si_2$ [19]	$\rho_0 - AT$	$a \ln(T_0/T)$	$a \ln(T_0/T)$	—
$U_{1-x}Th_xPd_2Al_3$ [9, 20]	$\rho_0 - AT$	$a \ln(T_0/T)$	$\chi_0 - A\sqrt{T}$	$(1/\tau_0)(1 - \omega/\omega_0)$
$Ce_{1-x}Th_xRhSb$ [21]	—	$a \ln(T_0/T)$	—	—
$U_xTh_{1-x}M_2Si_2$ (M = Ru, Pt, Pd) [22]	$\rho_0 + A \ln T$	$a \ln(T_0/T)$	$a \ln(T_0/T)$	—

There are a few scenarios that have been proposed to try to explain this anomalous behaviour. Some rely on the existence of a critical point at $T = 0$ [14]. Though these theories should be relevant to the cases of $CeCu_{6-x}Au_x$ and $CePd_2Si_2$ alluded to above, the alloys in table 1 are not obviously close to a phase boundary.

On the other hand, other proposals have focused on a local approach to the non-Fermi-liquid physics. These include exotic impurity models governed by a non-Fermi-liquid fixed point such as the quadrupolar Kondo model and various multi-channel Kondo models [23, 24]. These are largely based on the anomalous behaviour of a dilute system of such impurities. The inclusion of lattice effects presents an additional challenge that has only recently started to be addressed [25]. Another proposed route to non-Fermi-liquid behaviour has been to consider the competition between local charge and spin fluctuations [26]. It is quite possible, perhaps even likely, that the origin of the anomalous behaviour is different for different systems. We mention, in particular, the case of the last entry of table 1, $U_xTh_{1-x}M_2Si_2$ (M = Ru, Pt, Pd), whose description as a dilute system of magnetic two-channel impurities [23] in reference [22] appears to be fairly good.

The fact that the systems in table 1 are all disordered alloys immediately poses the question of the role of disorder in the formation of the non-Fermi-liquid state. Furthermore, recalling our operational definition of a Fermi liquid, one must not neglect the fact that the reference system in this case is almost certainly *a disordered one*. The behaviour of local moments in disordered systems has been considered in past studies [27–29].

In this paper, we will focus on the first alloy of the table, $UCu_{5-x}Pd_x$. The accumulated experimental data on this system have suggested to us that a model of disorder in f-electron systems is able to account for its anomalous behaviour. Of paramount importance to this conclusion was the Cu NMR study of reference [30], which detected a large inhomogeneous broadening of the NMR line, attributable to microscopic disorder. It is the goal of this paper to present a scenario in which a non-Fermi-liquid state is generated as a consequence of the interplay of disorder and strong correlations [31]. This theory provides a consistent way of understanding the non-Fermi-liquid anomalies in both transport and thermodynamic properties based on a single underlying mechanism. The central idea of this theory is that moderate bare disorder in a lattice model of localized moments is magnified due to the

strong local correlations between the moments and the conduction electrons. In particular, a broad distribution of local energy scales (Kondo temperatures) is generated [29]. A few local sites with very small Kondo temperatures are *unquenched* at low temperatures and dominate the thermodynamics and transport, forming a dilute gas of low-lying excitations above the disordered metallic ground state. The presence of these *unquenched* moments leads to the formation of a non-Fermi-liquid phase. While we think that $UCu_{5-x}Pd_x$ ($x = 1$ and $x = 1.5$) provides the best candidate system to exhibit such a phase to this date, we expect this type of behaviour to be seen in other Kondo alloys. Whether the other alloys in table 1 can be understood in this framework is not clear at this moment.

The outline of this paper is as follows. In section 2, we discuss the experimental work on the $UCu_{5-x}Pd_x$ alloys which served as the motivation for this study, emphasizing the most important underlying physical ideas. In section 3, we present the model and our dynamical mean-field-theory approach to its solution. In section 4, we show the nature of the ground state of the model in the clean as well as in the disordered limits. In section 5, we explain the origin of the linear dependence on the temperature of the resistivity. In section 6, we apply this disorder model to the description of the dynamical susceptibility and compare the results with experiments on $UCu_{5-x}Pd_x$. Finally, we conclude with a discussion of the limitations of our approach in section 7. In order to lighten the line of argument, a few derivations are left to the appendices.

2. The experimental basis for the disorder model

The major reason for considering disorder as the possible origin of the anomalous behaviour of the alloys of table 1 was the Cu NMR study reported in reference [30]. In this paper, the Cu NMR field-swept powder pattern spectra of $UCu_{5-x}Pd_x$ for $x = 1$ and $x = 1.5$ were shown to exhibit strong inhomogeneous broadening that could only be explained by invoking the presence of short-range disorder. A simple disorder model was then used to describe both the broadening of the NMR line and the spin susceptibility and specific heat measured in these samples. The model consisted of a collection of independent spins, mimicking the uranium ions, each coupled to the conduction electron bath by a dimensionless Kondo coupling constant $\lambda \equiv \rho_0 J$, which was allowed to be randomly distributed in the samples. These were supposed to mimic the local disorder induced by the Pd substitution in the Cu ligand sites of the parent UCu_5 compound and, for simplicity, were assumed to be distributed according to a Gaussian. Assuming that the spins were completely uncorrelated, the thermodynamic response was then calculated by taking an average over the response of a single Kondo spin with the distribution of coupling constants. Since the physics of a single Kondo spin is characterized by a single energy scale [3]—the Kondo temperature—the important quantity in the averaging procedure is the distribution of Kondo temperatures.

The Kondo temperature is defined as

$$T_K \equiv D e^{-1/\lambda}. \tag{2.1}$$

Because of the exponential dependence on the coupling constant λ, the corresponding distribution of Kondo temperatures is skewed and considerably broadened. Figure 1 shows the experimentally determined distributions of Kondo temperatures for both alloys ($x = 1$ and $x = 1.5$). We first note that, due to the Jacobian in the definition of $P(T_K)$, it actually diverges weakly as $T_K \to 0$:

$$P(T_K) = P[\lambda(T_K)]\left(\frac{d\lambda}{dT_K}\right) = \frac{P[\lambda(T_K)]}{T_K(\ln(D/T_K))^2}. \tag{2.2}$$
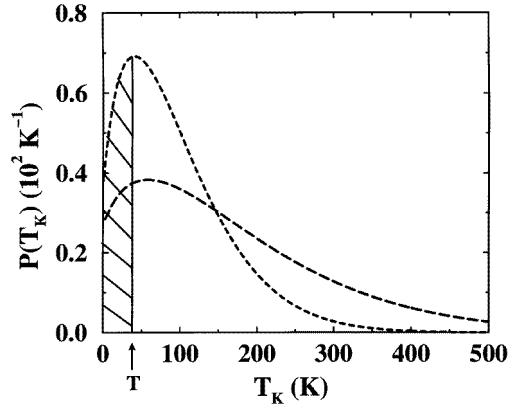
Figure 1. Experimentally determined distributions of Kondo temperatures of the alloys UCu$_{5-x}$Pd$_x$ with $x = 1$ (———) and 1.5 (– – –) (from reference [30]). The shaded area below T represents the low-T_K spins which remain unquenched at that temperature. The upturn at very low T_Ks is not shown (see the text for a discussion).

However, for the distributions determined experimentally for UCu$_{5-x}$Pd$_x$ ($x = 1$ and $x = 1.5$) and shown in figure 1, the point at which $P(T_K)$ shows an upturn and starts to diverge occurs at very low temperatures: $T_K \approx 2.4$ K ($x = 1$) and $T_K \approx 0.8$ K ($x = 1.5$), which can hardly be distinguished on the scale of figure 1. None of the conclusions derived from the use of the full $P(T_K)$ below depends on this small diverging tail, *as long as one does not probe into the low-temperature region below the upturn point scale*. Instead, as will be shown below, the response of the system is dominated by the part of $P(T_K)$ *above the upturn*, which appears to be tending to a constant value as $T_K \rightarrow 0$. This means that there are a finite number of spins with arbitrarily low T_Ks in the sample, a feature that will be at the root of the non-Fermi-liquid features. We have, therefore, chosen to depict $P(T_K)$ only above the upturn point and will confine the analysis below to a distribution which tends to a constant as $T_K \rightarrow 0$. It remains an interesting possibility whether the effects of the low-T_K divergence of $P(T_K)$ can be actually observed. On the other hand, it is also conceivable that there is a physical infrared cut-off λ_c to $P(\lambda)$ ($\lambda_c \lesssim 0.11$ for both distributions). In the absence of any experimental evidence for either possibility, we will focus on the more relevant effect of the distribution of Kondo temperatures above the upturn.

From the solution of the single-impurity Kondo problem it is known that thermodynamic quantities like the impurity spin susceptibility $\chi(T)$ increase with decreasing temperature in a Curie fashion, with logarithmic corrections [3]. However, at very low temperatures, the Curie-like divergence is cut off and the susceptibility saturates to a constant value proportional to the inverse Kondo temperature. The scale that separates the high-temperature from the low-temperature region is the Kondo temperature. The impurity specific heat divided by the temperature $C_V(T)/T$ has a somewhat similar behaviour. The saturation at the lowest temperatures is a consequence of the 'disappearance' of the free-spin response, through the formation of a singlet ground state with the conduction electron bath, a process generally known as 'quenching'.

If we are measuring the thermodynamic properties at a certain finite temperature T, there will always be uranium ions with $T_K < T$, which remain unquenched and whose contribution dominates the overall response (the shaded area in figure 1). As the temperature is lowered, the number of such spins decreases, as more and more of them become quenched. The

thermodynamic behaviour of the disordered system is, therefore, dominated by the tails of the distribution of Kondo temperatures, rather than by the average, a situation commonly known as a Griffiths phase [32].

Since both $\chi(T)$ and $C_V(T)/T$ scale as the inverse Kondo temperature at $T = 0$, the fact that $P(T_K = 0) \neq 0$ immediately implies that the leading behaviour of the averaged quantity is a logarithmic divergence. Indeed, consider, for example, the susceptibility

$$\chi(T) \propto \frac{1}{T_K} f\left(\frac{T}{T_K}\right) \tag{2.3}$$

where the asymptotic forms of $f(x)$ are known [3]:

$$f(x) \approx \begin{cases} \alpha - \beta x^2 & x \ll 1 \\ \dfrac{\gamma}{x}\left(1 - \dfrac{1}{\ln x}\right) & x \gg 1 \end{cases} \tag{2.4}$$

where α, β and γ are universal numbers. To find the leading low-temperature behaviour it is sufficient to use the first term in $P(T_K) = P_0 + P_1 T_K + \cdots$. Therefore, if $\langle \cdots \rangle^{\mathrm{av}}$ denotes the average over the distribution of Kondo temperatures,

$$\langle \chi(T) \rangle^{\mathrm{av}} \propto \int_0^\infty \frac{\mathrm{d}T_K}{T_K} \, P(T_K) f\left(\frac{T}{T_K}\right) \approx \int_0^{\Gamma/T} \frac{\mathrm{d}y}{y} \, P_0 f(1/y) \tag{2.5}$$

where we cut off the integral by an arbitrary scale Γ which sets the region of validity of the approximate form for $P(T_K)$. From (2.4), it is clear that the lower limit of the integral in (2.5) gives a regular contribution whereas the upper limit dominates:

$$\langle \chi(T) \rangle^{\mathrm{av}} \approx \int^{\Gamma/T} \frac{\mathrm{d}y}{y} \, \alpha P_0 \sim \alpha P_0 \ln\left(\frac{\Gamma}{T}\right). \tag{2.6}$$

A similar analysis holds for $C_V(T)/T$, with a similar divergence.

A caveat about the experimental situation is in order here. In the literature, one often finds different power laws fitted to thermodynamic and transport properties of this and other compounds. In the particular case of $UCu_{5-x}Pd_x$, one can find $\chi(T) = \chi_0 T^{-\eta}$, with $\eta = 0.27 \pm 0.03$ [15], $\eta = 0.25$ [9] and $\eta = 1/3$ [24, 33]. It is not always clear what temperature range was used in the fits. In the case of reference [24], the $\eta = 1/3$ power law is argued to be valid in an intermediate range of temperatures (between 20 and 300 K). Besides, there is a small sample dependence to these quantities and, in the case of the susceptibility, the magnetic field strength used in the measurement can have an important effect [30]. We feel that all these aspects should be carefully considered when trying to determine the temperature dependence.

It is important to notice that the distribution of Kondo temperatures reported in reference [30], which is nearly featureless at low T_K, gives a logarithmic divergence in $\chi(T)$ and $C_V(T)/T$ as the *leading* low-temperature behaviour. In the fits shown in reference [30], there are clear deviations from this leading behaviour at intermediate and higher temperatures. We point out that power-law behaviour could be inferred from the analysis of a narrow window of temperatures. What gives us particular confidence in the disorder model is the fact that a full theoretical curve, with the added complication of a finite magnetic field, can be well fitted to the experiments. On the other hand, it is not clear how changes in the specific form of the distribution function used would affect the quality of the fit in the intermediate and high-temperature regions.

Finally, for completeness, we have plotted in figure 2 the Wilson ratio $(R_W \equiv T\chi(T)/C_V(T))$ prediction in the disorder model as a function of temperature.
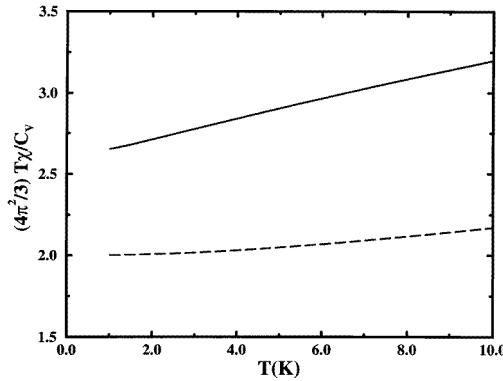
Figure 2. The Wilson ratio as a function of temperature as predicted by the disorder model for the cases where $P(T_K = 0) \neq 0$ (———) and $P(T_K = 0) = 0$ (– – –). Note how the latter tends to the universal zero-temperature value of 2.

When $P(0) = 0$, the Wilson ratio tends to its universal value of 2 when $T \to 0$, which is consistent with the Fermi-liquid prediction. When $P(0) \neq 0$, the Wilson ratio appears to tend to a different value for a wide range of temperatures. This can be understood from (2.6). Because the scale Γ, which enters this equation, depends on the details of the full scaling curve, it is going to be, in general, different for $\chi(T)$ as compared to $C_V(T)/T$. Though the scale is asymptotically irrelevant when $T \gg \Gamma$, because of the slow logarithmic dependence, it takes a temperature that is too low for one to be able to observe the asymptotic behaviour.

We point out that one feature which distinguishes the alloy $UCu_{5-x}Pd_x$ from the other alloys in table 1 is the nature of the doping. In the former case, the f sublattice remains unchanged and substitutions are introduced in the ligand sites. In the other cases, the doping is performed directly in the f sites. It is apparent that ligand site substitution will affect the hybridization matrix element V of an Anderson model description and that will probably be the primary effect (see section 3 for a discussion of the disordered Anderson lattice model). It is less certain what kind of effect such substitution will have on the f-site energy E^f. Moreover, lattice microstrains should also be reflected in the hybridization amplitude V. This is probably what happens in UCu_4Pd, which could be stoichiometric and indeed appears to be so according the x-rays, but whose broad NMR lines give unequivocal evidence of disorder. On the other hand, f-site replacements can be mimicked by a different f-site energy E^f ($E^f \to +\infty$, when the substitutional ion is a non-magnetic 'Kondo hole') and, presumably, a different hybridization V. In the interest of generality, and in the absence of a better understanding of the nature of the disorder, we will consider in this paper *both* E^f- and V-disorder. What should be emphasized, however, is the fact that, *whatever the microscopic origin of the disorder*, its observable consequences will always depend only on the distribution of Kondo temperatures $P(T_K)$, for it is these scales which govern the measured responses. In other words, almost all of the information that can be obtained experimentally about the disorder will be filtered through $P(T_K)$.

Therefore, the main conclusion of reference [30] was that a simple model of Kondo disorder is able to account for the NMR line broadening as well as the anomalous thermodynamic response of the alloys studied. This simple model relied on the assumption that the correlations between the Kondo spins could be neglected, though they form

a concentrated lattice in these alloys. Past studies of heavy-fermion systems, both experimental [34] and theoretical [35], give us confidence that this may not be a bad approximation for thermodynamic quantities (see also the appendix C). However, it is well known that transport is *very* different in dilute Kondo systems as opposed to concentrated Kondo lattices. The so-called onset of coherence in the clean, concentrated case is the most dramatic example. It is characterized by rather large resistivities at high and intermediate temperatures, a consequence of strong incoherent Kondo scattering off the localized moments, which is then followed by a precipitous fall by some orders of magnitude at the lowest temperatures. At very low temperatures, the system can then be characterized as a good metal. This low-temperature coherence is a consequence of translational invariance and Bloch's theorem in the ordered lattice system. We will, therefore, address the question of whether a single unifying approach to the disorder problem, sensitive enough to the formation of a coherent state in the clean limit, is able to be formulated. We will answer the latter question in the affirmative and will thereby show that the same mechanism that leads to diverging thermodynamic properties at low T—the presence of spins with arbitrarily low T_Ks—will also predict a resistivity which is *linear* in T, as observed in many non-Fermi-liquid heavy-fermion alloys.

3. The disordered Anderson lattice model and the dynamical mean-field-theory equations

In order to consider the interplay of disorder and local moment behaviour we will focus our attention on a model of disordered Anderson lattices. We will be guided by the series of alloys listed in table 1. In the spirit of previous works on heavy-fermion systems we will assume that the f-electron sites can be described by simplified non-degenerate Anderson impurities hybridized with a single broad uncorrelated band of conduction electrons:

$$H = \sum_{k\sigma} \epsilon(k) c_{k\sigma}^{\dagger} c_{k\sigma} + \sum_{j\sigma} E_j^f f_{j\sigma}^{\dagger} f_{j\sigma} + \sum_{j\sigma} (V_j c_{j\sigma}^{\dagger} f_{j\sigma} + \text{HC}) + U \sum_j n_{fj\uparrow} n_{fj\downarrow} \tag{3.1}$$

where, $c_{k\sigma}$ destroys a conduction electron with momentum k and spin σ from a band with dispersion $\epsilon(k)$ and half-bandwidth D, and $f_{j\sigma}$ destroys an f electron at site j with spin σ. Since U is generally the largest energy scale in typical f-shell parameters it will be taken to infinity in this paper.

The important thing to notice in (3.1) is that, unlike in the usual periodic Anderson model, the local f-shell parameters E_j^f and V_j are taken here to be random numbers distributed, in general, according to two different distributions $P_1(E^f)$ and $P_2(V)$. As explained before, in the absence of a more detailed understanding of the microscopic nature of the disorder in these systems, one should take $P_1(E^f)$ and $P_2(V)$ to be, in principle, of the most general form. Note, however, that we will *not* assume the disorder widths to be too large. For instance, the NMR study of reference [30] suggests bare distribution widths to be around 20% of their average values. However, as we will see, correlation effects will themselves generate large *effective* disorder. In practice, we have considered Gaussian and uniform distributions. Disorder in the conduction electron band, though certainly present in these alloys, is not subject to these correlation-induced renormalizations and has therefore been neglected in our treatment. Despite these simplifications, we believe that the model in (3.1) captures the essential ingredients relevant to the study of disorder in Kondo alloys.

Some previous studies of disordered Anderson or Kondo lattices have been reported in the literature. We mention, in particular, the early work of Tešanović, who employed a

slave-boson approach [36]. More recently, other studies of the effect of disorder in these model systems have appeared [37, 38].

In order to make progress, we have applied the dynamical mean-field theory of correlations and disorder to the Hamiltonian of (3.1) [39–41]. The derivation of the dynamical mean-field theory is most easily accomplished on a Bethe lattice and we will focus on this class of models. In this case, the conduction electron density of states acquires a simple semicircular form. The solution of the full lattice problem then reduces to the solution of an *ensemble* of impurity problems supplemented by a self-consistency condition on the conduction electron Green's function [41]. More precisely, the impurity problem action for a random site j is given, on the Matsubara frequency axis, by

$$S_j^{\text{imp}} = T \sum_{\omega_n \sigma} [f_{j\sigma}^\dagger(\mathrm{i}\omega_n)(-\mathrm{i}\omega_n + E_j^f + V_j^2 \Delta(\mathrm{i}\omega_n)) f_{j\sigma}(\mathrm{i}\omega_n)] \tag{3.2}$$

where the infinite-U constraint is implied and

$$\Delta(\mathrm{i}\omega_n) = \frac{1}{\mathrm{i}\omega_n + \mu - t^2 \overline{G}_c(\mathrm{i}\omega_n)}. \tag{3.3}$$

Here, t is the conduction electron hopping matrix element and $\overline{G}_c(\omega)$ is the disorder-averaged local conduction electron Green's function. Note that $\Delta(\mathrm{i}\omega_n)$ is the hybridization function of the conduction electrons which is 'seen' by each local f site. Therefore, it corresponds to the local conduction electron Green's function with one f site removed. This is the so-called 'cavity' Green's function [41].

The self-consistency condition determines $\overline{G}_c(\omega)$ through

$$\overline{G}_c(\mathrm{i}\omega_n) = \left\langle \frac{1}{\mathrm{i}\omega_n + \mu - t^2 \overline{G}_c(\mathrm{i}\omega_n) - \Phi_j(\mathrm{i}\omega_n)} \right\rangle^{\text{av}} \tag{3.4}$$

where

$$\Phi_j(\mathrm{i}\omega_n) = \frac{V_j^2}{\mathrm{i}\omega_n - E_j^f - \Sigma_{fj}^{\text{imp}}(\mathrm{i}\omega_n)}. \tag{3.5}$$

Here, $\langle \ldots \rangle^{\text{av}}$ denotes the average over disorder defined by the distribution functions $P_1(E^f)$ and $P_2(V)$. $\Sigma_{fj}^{\text{imp}}(\mathrm{i}\omega_n)$ is the f-electron self-energy derived from the impurity model of (3.2). This is explicitly defined by

$$\Sigma_{fj}^{\text{imp}}(\mathrm{i}\omega_n) = \mathrm{i}\omega_n - E_j^f - V_j^2 \Delta(\mathrm{i}\omega_n) - G_{fj}^{\text{imp}}(\mathrm{i}\omega_n) \tag{3.6}$$

where the f-electron Green's function is given by

$$\begin{aligned} G_{fj}^{\text{imp}}(\tau) &= -\langle T f_j(\tau) f_j^\dagger(0) \rangle_j^{\text{imp}} \\ G_{fj}^{\text{imp}}(\mathrm{i}\omega_n) &= \int_0^\beta \mathrm{d}\tau \; G_{fj}^{\text{imp}}(\tau) \mathrm{e}^{\mathrm{i}\omega_n \tau}. \end{aligned} \tag{3.7}$$

Here, we have used $\langle \ldots \rangle_j^{\text{imp}}$ to denote the quantum mechanical/thermal average under the action of (3.2).

Once the problem defined by (3.2)–(3.7) has been solved, the conduction electron self-energy $\Sigma_c(\mathrm{i}\omega_n)$ is obtained from

$$\overline{G}_c(\mathrm{i}\omega_n) = \int_{-2t}^{2t} \mathrm{d}\epsilon \; \frac{\rho_0(\epsilon)}{\mathrm{i}\omega_n + \mu - \epsilon - \Sigma_c(\mathrm{i}\omega_n)} \qquad \rho_0(\epsilon) = \frac{1}{\pi t}\sqrt{1 - (\epsilon/2t)^2}. \tag{3.8}$$

This self-energy is the important object for the calculation of the conductivity, which, in the infinite-coordination limit, involves no vertex corrections [42]:

$$\sigma(\omega) = \frac{(2te)^2}{\hbar \pi a} \int_{-\infty}^{+\infty} d\nu \int_{-\infty}^{+\infty} d\epsilon \; \frac{f(\nu) - f(\nu + \omega)}{\omega} \rho_0(\epsilon) A(\epsilon, \nu) A(\epsilon, \nu + \omega) \qquad (3.9)$$

where $f(\nu)$ is the Fermi function and we have introduced a lattice parameter a and the correct dimensional factors appropriate for three dimensions. In (3.9), $A(\epsilon, \omega)$ is the conduction electron one-particle spectral density

$$A(\epsilon, \omega) = \operatorname{Im} G_c(\epsilon, \omega) \equiv \operatorname{Im}\left(\frac{1}{\omega + \mu - \epsilon - \Sigma_c(\omega)}\right). \qquad (3.10)$$

The DC conductivity is then given by

$$\sigma_{DC} = \frac{(2te)^2}{\hbar \pi a} \int_{-\infty}^{+\infty} d\nu \left(-\frac{\partial f}{\partial \nu}\right) \int_{-\infty}^{+\infty} d\epsilon \; \rho_0(\epsilon) A^2(\epsilon, \nu). \qquad (3.11)$$

This expression can be further simplified as shown in appendix A. To make contact with the usual Drude formula for the DC conductivity it is useful to define the scattering time

$$\tau \equiv \frac{1}{\pi \rho_0(\mu)} \int_{-\infty}^{+\infty} d\nu \left(-\frac{\partial f}{\partial \nu}\right) \int_{-\infty}^{+\infty} d\epsilon \; \rho_0(\epsilon) A^2(\epsilon, \nu) \qquad (3.12)$$

which reduces to the usual case when $\tau \gg 1/D$:

$$\tau \longrightarrow \frac{1}{2 \operatorname{Im} \Sigma_c(0)} \qquad (\tau \gg 1/D). \qquad (3.13)$$

In appendix B, a formula which expresses the conduction electron self-energy in terms of the disorder-averaged impurity T-matrix is derived. This formula will be useful in section 5, when we analyse the temperature dependence of the resistivity.

Thermodynamic properties within this approach are not drastically different from the predictions of the simple disorder model of reference [30], discussed in section 2. Though the self-consistently determined conduction electron density of states 'seen' by the f sites ($\Delta(\omega)$) can be substantially modified as compared to its free value, these modifications only lead to a renormalized density of states, which is the quantity that ultimately enters into the Kondo temperature expression. Once the renormalized density of states is given, the prediction of the dynamical mean-field theory is essentially the same as that of the simple disorder model of reference [30], the difference being negligible. We discuss the thermodynamics properties in the dynamical mean-field theory in appendix C.

We would like to emphasize at this point what processes are included and what processes are left out of this approach. When the interaction U is turned off, the treatment of the disorder problem that is obtained is equivalent to the well-known coherent-potential approximation (CPA) [43]. This approximation is known to give reliable results as long as localization effects are negligible, since the conduction electron density-of-states fluctuations are treated on average. This seems to be a safe approximation in the case of the alloys of interest, where estimates based on the zero-temperature DC resistivity give $k_F l \approx 3$–10. However, the interplay of disorder fluctuations and correlations on the f sites is fully kept in our treatment and, indeed, is at heart of the physics that will emerge. This is evident from the fact that one needs to correctly solve an *ensemble* of interacting impurity problems in order to close the equations. Each member of the *ensemble* of impurity problems has an associated characteristic Kondo temperature T_K, thus generating a distribution of local Kondo scales [29]. The fluctuations associated with this distribution of Kondo temperatures will be responsible for the anomalous low-temperature behaviour in the non-Fermi-liquid

regime. Other processes which are left out of this essentially local approach are related to the RKKY interaction between f sites mediated by the exchange of conduction electron spin fluctuations. We will comment on the possible limitations of this approximation in section 7.

4. The zero-temperature state

The most difficult part of solving (3.2)–(3.7) is solving the impurity problem. Let us consider initially the clean case. Then, there is only one impurity model to be solved. Equations (3.4) and (3.8) are then trivially solved and yield $\Sigma_c(\omega) = \Phi(\omega)$. At low temperatures, the impurity problem is governed by a Fermi-liquid fixed point [3, 4] and $\Sigma_f^{\mathrm{imp}}(\omega)$ can be parametrized at low temperatures and energies as [44]

$$\Sigma_f^{\mathrm{imp}}(\omega) \approx a + b\omega + \mathrm{i}c(\omega^2 + \pi^2 T^2) \tag{4.1}$$

where, a, b and c are constants. From this, it follows that

$$\Sigma_c(\omega) \approx \frac{zV^2}{\omega - \tilde{\epsilon}_f - \mathrm{i}zc(\omega^2 + \pi^2 T^2)} \tag{4.2}$$

where we have redefined a and b in terms of a renormalized f-level energy $\tilde{\epsilon}_f$ and a wave-function renormalization factor z. The first thing to notice in this expression is that at $T = 0$, $\Sigma_c(0)$ is real, leading to a purely real conduction electron self-energy in the pure case. This is the hallmark of the low-temperature coherent transport of the clean system, a consequence of translational invariance and a feature naturally incorporated in the dynamical mean-field theory. Furthermore, the Fermi-liquid form of the impurity problem self-energy ultimately leads to the Fermi-liquid behaviour of the conduction electron lattice self-energy. In particular, the resistivity derived from (4.2) will exhibit a characteristic T^2-law.

Let us now move on to the disordered case at zero temperature. We have employed the slave-boson mean-field theory to solve the *ensemble* of impurity problems at $T = 0$ [35]. This theory is known to provide a good description of the infinite-U Anderson impurity model at temperatures $T \ll T_K$. It will also serve as a good starting point for the understanding of the complete solution of our dynamical mean-field equations at an arbitrary temperature. Details of the slave-boson treatment of the impurity problem are given in appendix D. These solutions to the *ensemble* of impurity problems were then used in an iteration scheme to solve the full set (3.2)–(3.7).

Figure 3 shows the self-consistent solution to $G_c(\omega)$ in the clean case and figure 4 shows the corresponding 'cavity' Green's function $\Delta(\omega)$. The only modification introduced by the lattice of f sites to the conduction electron density of states is the appearance of a gap centred around the renormalized f-level position ϵ_f. This is familiar from the slave-boson large-N solution of the infinite-U Anderson lattice [35]. The scale of the gap is given by $\approx r^2 V^2/D$, which is the Kondo temperature scale. The important feature of the imaginary part of the 'cavity' Green's function $\Delta(\omega)$ is the appearance of a delta function at the centre of the gap ϵ_f, which corresponds to the removal of one f site.

The presence of disorder introduces important changes in these structures at the scales given by the range of Kondo temperatures produced as a consequence of the distribution of local f parameters. These are defined here as

$$T_{Kj} \equiv \sqrt{(\epsilon_j^f - \tilde{\Delta}_j'(0))^2 + (\tilde{\Delta}_j''(0))^2} \tag{4.3}$$
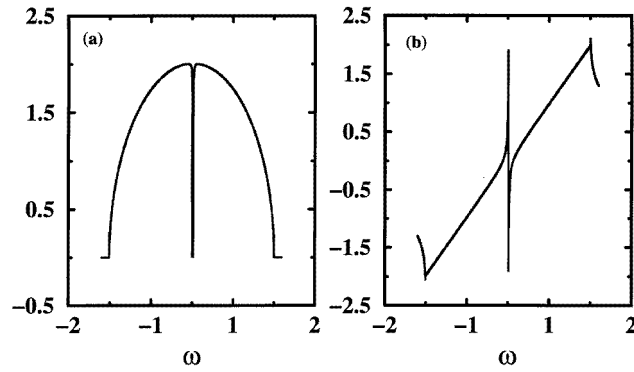
Figure 3. (a) Imaginary and (b) real parts of the conduction electron local Green's function as a function of frequency at $T = 0$. The parameters used were: $D = 1$, $V = 0.1$, $\mu = 0$, $E^f = -0.05$, and there is no disorder.
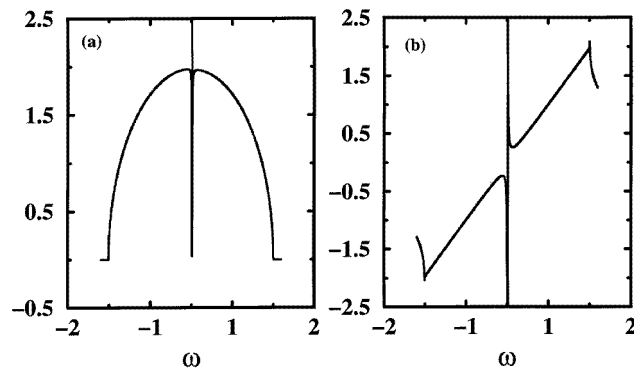

Figure 4. (a) Imaginary and (b) real parts of the conduction electron 'cavity' Green's function $\Delta(\omega)$ (see (3.3)) as a function of frequency at $T = 0$. The parameters used were: $D = 1$, $V = 0.1$, $\mu = 0$, $E^f = -0.05$, and there is no disorder.

where $\tilde{\Delta}_j(\omega) \equiv r_j^2 V_j^2 \Delta(\omega)$ and we are denoting real and imaginary parts by single and double primes, respectively. In the Kondo limit, they acquire the familiar form

$$T_{Kj} \rightarrow D \exp\left(E_j^f / (2\rho_0 V_j^2)\right) \tag{4.4}$$

where $\rho_0 = \Delta''(0)/\pi$. Figure 5 shows a typical distribution of Kondo temperatures from a fully self-consistent solution of the zero-temperature problem. For comparison, we have also plotted the $P(T_K)$ used in the fit to the susceptibility of UCu$_4$Pd in reference [30]. The self-consistent distribution has a structure very similar to the experimentally determined one.

These modifications are illustrated in figures 6, 7 and 8, which show the influence of various amounts of disorder on the gap structure of $G_c(\omega)$ and $\Delta(\omega)$. Only the low-energy region is shown since that is the only region that is strongly influenced by the introduction of disorder. It is clear from figure 6 that sufficient disorder can close the gap in the conduction electron density of states. Qualitatively, a distribution of Kondo energy scales for the *ensemble* of impurity problems will be reflected in a distribution of energy gaps. Their sizes and positions are essentially determined by the T_{Kj}s and ϵ_j^fs, respectively,
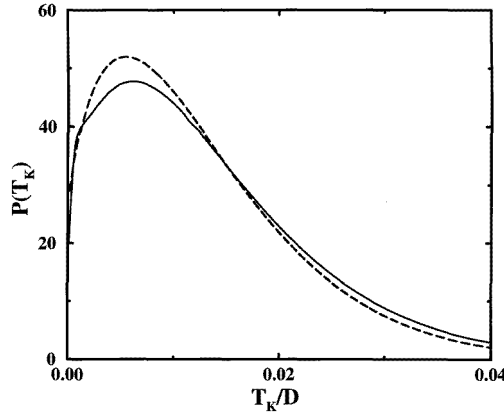
Figure 5. A typical distribution of Kondo temperatures obtained in the fully self-consistent solution of the dynamical mean-field theory (——) and the distribution appropriate for UCu$_4$Pd from reference [30] (– – –). The distribution was a Gaussian and the parameters used were: $D = 1$, $\mu = 0$, $E^f = -1$, $\langle V^2 \rangle = 0.17$, $W_{V^2} = 0.032$. The upturn at very low T_Ks is not shown.
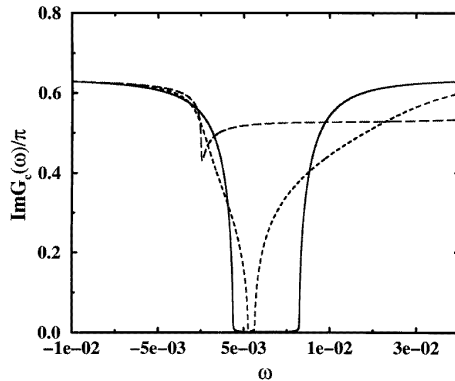

Figure 6. The imaginary part of the conduction electron Green's function as a function of frequency at $T = 0$ for different amounts of disorder in the E^f-parameter. A uniform distribution was used with widths $W = 0.001$ (——), $W = 0.05$ (– – –) and $W = 0.15$ (— — —). The parameters used were: $D = 1$, $V = 0.1$, $\mu = 0$, $\langle E^f \rangle = -0.05$.
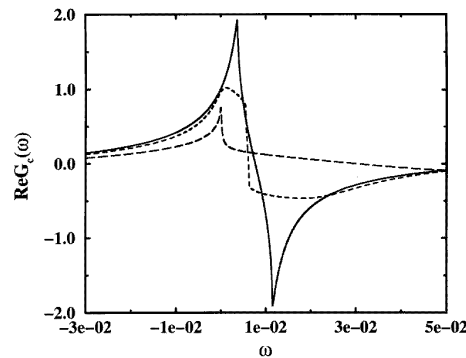
Figure 7. The real part of the conduction electron Green's function as a function of frequency at $T = 0$ for different amounts of disorder in the E^f-parameter. A uniform distribution was used with widths $W = 0.001$ (——), $W = 0.05$ (– – –) and $W = 0.15$ (— — —). The same parameters were used as in figure 3.

and sufficient disorder in their distributions will lead to an ultimate closing of the gap. In the metallic regime being considered here, the disappearance of the gap does not lead to dramatic effects, since the chemical potential lies away from the gap region. However, there might be important consequences in the Kondo insulator or Anderson insulator regimes. Corresponding modifications are also present in the real parts of $G_c(\omega)$ and $\Delta(\omega)$, as seen in figures 7 and 8. The result is similar in the case where E^f is uniform and V_j is distributed, since the relevant scales are the Kondo temperatures (4.4). However, due to the different dependences of T_{Kj} on E^f_j and V_j, their distributions will be quantitatively different and will reflect differently on the T_{Kj}-distribution and consequently on the transport properties.
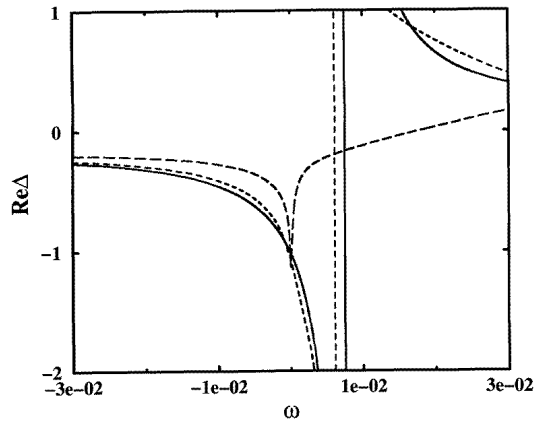
Figure 8. The real part of the conduction electron 'cavity' Green's function $\Delta(\omega)$ as a function of frequency at $T = 0$ for different amounts of disorder in the E^f-parameter. A uniform distribution was used with widths $W = 0.001$ (——), $W = 0.05$ (– – –) and $W = 0.15$ (— — —). The same parameters were used as in figure 3.

The central aspect of the interplay between disorder and correlations is an *enhancement* of the bare disorder by the local Kondo physics of the impurity *ensemble*. This can be quite easily understood by an examination of the qualitative aspects of the solution at $T = 0$. At zero temperature, only $\Phi_j(0)$ enters into the calculation of $\Sigma_c(0)$ or $G_c(0)$, either of which, in turn, is enough for the calculation of the DC conductivity (see (3.11) or (A.3)). As was emphasized before, given a certain distribution of the quantities Φ_j, equation (3.4) corresponds to a CPA treatment of disorder in the conduction band, where the Φ_js play the role of scattering potential strengths. Interactions are important in determining the value that these latter quantities acquire, given a self-averaged conduction electron bath through $\Delta(\omega)$.
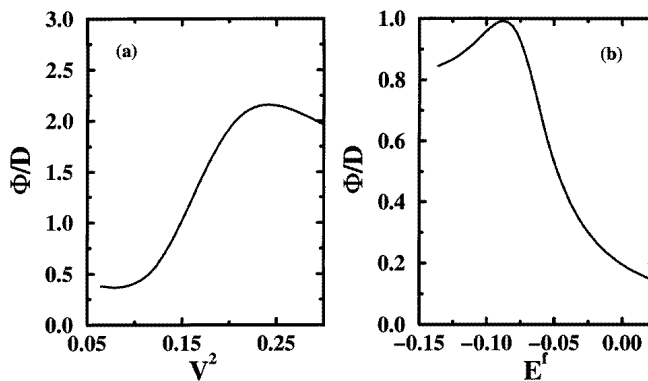

Figure 9. The variation of the effective local scattering potential strength $\Phi(0)$ as a function of V^2 and E^f. Notice how $\Phi(0)$ varies on the scale of conduction electron parameters (D) *not* on the scale of local f parameters. The distributions used were Gaussian and the parameters were $D = 1$, $\mu = 0$, (a) $E^f = -1$, $\langle V^2 \rangle = 0.17$, $W_{V^2} = 0.032$, (b) $V = 0.1$, $\langle E^f \rangle = -0.055$ and $W_{E^f} = 0.027$.

From the Fermi-liquid analysis, the zero-temperature, zero-energy form of $\Phi_j(0)$ is real and given by

$$\Phi_j(0) = -\frac{V_j^2}{E_j^f + \Sigma_j^{\text{imp}}(0)}. \tag{4.5}$$

In the slave-boson mean-field theory, it is given by (see (D.11))

$$\Phi_j(0) = -\frac{r_j^2 V_j^2}{\epsilon_j^f}. \tag{4.6}$$

Now, in the Kondo limit $|E_j^f| \gg \rho_0 V_j^2$ ($E_j^f < 0$), it is easy to show from the mean-field equations (D.7) and (D.8) that

$$\Phi_j(0) \longrightarrow \frac{1}{\Delta'(0)} \qquad (|E_j^f| \gg \rho_0 V_j^2, E_j^f < 0). \tag{4.7}$$

The important point here is the fact that the impurity problem parameters have disappeared from the local effective scattering potential strength and its scale is now given by the conduction electron band scale. As can be seen from figure 8, the real part of the 'cavity' Green's function that enters (4.7) spans a wide range of values in the region close to the chemical potential (here set to zero). Because of the distribution of local parameters ϵ_j^f and r_j, this whole region close to μ will be probed by the different f sites and $\Phi_j(0)$ will also vary. However, its variation will be on the conduction electron scale. Indeed, we have plotted in figure 9 the variation of $\Phi_j(0)$ for a given strength of disorder, in both cases of random E_j^fs and random V_js. It is clear that its distribution range is *not* on the same scale as the variation of local f parameters, which is very narrow, but rather, on the scale of D. *Therefore, the effective disorder seen by the conduction electrons is considerably enhanced due to the local f-shell correlation effects.*
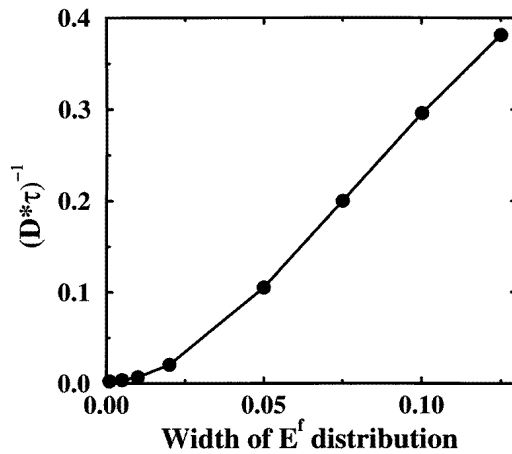

Figure 10. The scattering rate as a function of the width of the uniform E^f-distribution. The strong correlations in the f shell produce an enhanced effective disorder. The parameters used were: $D = 1$, $\mu = 0$, $V = 0.1$, $\langle E^f \rangle = -0.05$.

As a result of this enhancement effect, large resistivities can be generated even though the range of variation of the f-shell parameters is very narrow. This is illustrated in figure 10, where the scattering rate $1/\tau$, as given from (3.12), is plotted as a function

of the width of the uniform E^f-distribution. It is clear that modest amounts of disorder in E^f produce rather substantial scattering rates. Thus, although the clean system exhibits coherent transport at low T, *the introduction of a small amount of f-site disorder leads to the destruction of these coherence effects.* Qualitatively, once the lattice effects of coherence are destroyed by sufficient disorder, the resistivity as a function of temperature will then resemble the independent Kondo impurity results, with its characteristic decreasing resistivity with increasing temperature. This point was nicely illustrated in a recent study [38] of binary alloy disorder in the Anderson lattice, which relies on a similar treatment of correlations and disorder. Furthermore, several doping studies of heavy-fermion systems seem to bear out the above picture [34].

We summarize now the two major results of the study of disorder discussed in this section.

- Due to the local Kondo physics at each f site, the *effective* disorder generated from a bare distribution of local f-shell parameters is strongly renormalized up to scales of the order of the conduction electron bandwidth.
- Although the clean system has low resistivities due to the onset of coherence at low T, moderate amounts of f-shell disorder are capable of destroying this low-T coherence, leading to characteristic incoherent Kondo scattering behaviour.

5. The linear temperature dependence of the resistivity

Having established the incoherent nature of the transport with sufficient disorder strength, we now focus on the temperature dependence of the resistivity in this strongly correlated disordered state. We will rely on appendix B, which relates the conduction electron self-energy $\Sigma_c(\omega)$ to the averaged impurity model T-matrix $T_j^{\text{imp}}(\omega)$ (equation (B.4)). At sufficiently high temperatures, compared to the highest T_K in the distribution, the averaged T-matrix at low energies becomes very small, reflecting the weak-coupling nature of the impurity response at high temperatures. Therefore, there will be only a small contribution to the conduction electron self-energy and consequently to the resistivity. At zero temperature, as discussed in section 4, sufficient disorder will kill all coherence in the transport properties and the system will exhibit a rather large resistivity. What happens at low temperatures?

For that, it is convenient to analyse the average impurity T-matrix. We have therefore plotted in figure 11 the imaginary part of the impurity T-matrix, using the distribution of Kondo temperatures derived from the fit to the thermodynamic properties of $\text{UCu}_{5-x}\text{Pd}_x$ [30]. It is clear that the leading temperature dependence is linear. This leads to a linear conduction electron self-energy and to a linear resistivity through (3.11), consistent with the behaviour observed in several of the alloys in table 1. At higher temperatures, there are clear deviations from the leading linear behaviour as can be seen in the inset. Can we understand what conditions are necessary for this anomalous non-Fermi-liquid behaviour?

The essential condition for the linear temperature dependence of the resistivity, like the thermodynamic response discussed in section 2, is that the distribution of Kondo temperatures be such that $P(T_K = 0) \neq 0$. In other words, there must be a finite fraction of f sites with arbitrarily small Kondo temperatures. This can be made more apparent by an analysis similar to the one in section 2. However, one has to be careful of how one understands the averaging process. This is because, unlike the thermodynamic responses, transport properties *cannot be averaged over single-impurity results.* This is made evident in the analysis of the zero-temperature state of section 4. The single-impurity result amounts to a strong, almost unitary scattering centre at $T = 0$, with a correspondingly large resistivity.
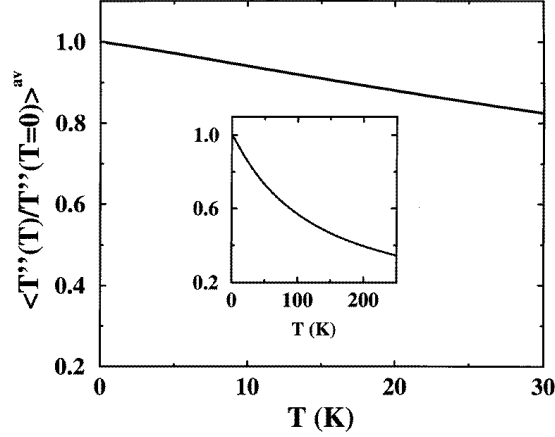
Figure 11. The temperature dependence of the imaginary part of the single-impurity T-matrix averaged over the disorder distribution appropriate for UCu$_{3.5}$Pd$_{1.5}$, as determined experimentally in reference [30]. The inset shows the same quantity over a wider temperature range.

Any attempt to simply average this result would lead to a large resistivity. However, due to translational invariance, it is clear that the clean sample can only have a vanishing resistivity, a result which encounters a natural description in the dynamical mean-field theory, as was explained. Even in the disordered case, only the CPA-like averaging process embodied in (3.4) has any sense. However, given a disordered ground state, *deviations from zero temperature* can still be analysed in a fashion that resembles the averaging of thermodynamic quantities. This is because, at low temperatures, a few low-T_K spins are unquenched and cease to contribute significantly to the scattering. Since they form a *dilute* system of subtracted scattering centres, their contribution is additive and can therefore be averaged.

With these caveats in mind, we can proceed to analyse the conduction electron self-energy. If the temperature is raised from 0 to T, there will be corresponding variations in all quantities. From (B.3),

$$\delta\Sigma_c(\omega) = \left.\frac{1 - t^2 G_c^2(\omega)}{G_c^2(\omega)}\right|_{T=0} \delta G_c(\omega) \tag{5.1}$$

and $\delta G_c(\omega)$ can be obtained from (B.2):

$$\left\{t^2 + \left[\omega - t^2 G_c(\omega)\right]\left[\omega - 3t^2 G_c(\omega)\right]\right\}\big|_{T=0} \delta G_c(\omega) = \delta\langle T_j^{\mathrm{imp}}(\omega)\rangle^{\mathrm{av}}. \tag{5.2}$$

At this point it is useful to remember the definition of the T-matrix (see (B.1) and (3.6)):

$$T_j^{\mathrm{imp}}(\omega) = \frac{V_j^2}{\omega - E_j^f - V_j^2/\left[\omega - t^2 G_c(\omega)\right] - \Sigma_{fj}^{\mathrm{imp}}\left[\omega, T, G_c\right]}. \tag{5.3}$$

In (5.3) we have highlighted the fact that $\Sigma_{fj}^{\mathrm{imp}}$ is a functional of $G_c(\omega)$ as well as a function of ω and T. Therefore, it is clear that the T-matrix depends on the temperature through $\Sigma_{fj}^{\mathrm{imp}}$. However, since $G_c(\omega)$ changes with temperature, we also need to take into account this additional contribution, both explicitly and implicitly through $\Sigma_{fj}^{\mathrm{imp}}$. We therefore,

separate three different contributions:

$$\delta T_j^{\text{imp}}(\omega) = \delta_1 T_j^{\text{imp}}(\omega) + \delta_2 T_j^{\text{imp}}(\omega) + \delta_3 T_j^{\text{imp}}(\omega) \tag{5.4}$$

$$\delta_1 T_j^{\text{imp}}(\omega) = \left. \frac{t^2 (T_j^{\text{imp}}(\omega))^2}{\left[\omega - t^2 G_c(\omega)\right]^2} \right|_{T=0} \delta G_c(\omega) \tag{5.5}$$

$$\delta_2 T_j^{\text{imp}}(\omega) = \left. \delta_T T_j^{\text{imp}}(\omega) \right|_{G_c^0} \tag{5.6}$$

$$\delta_3 T_j^{\text{imp}}(\omega) = \frac{(T_j^{\text{imp}}(\omega))^2}{V_j^2} \int \mathrm{d}\omega' \left. \frac{\delta \Sigma_{fj}^{\text{imp}}(\omega)}{\delta G_c(\omega')} \right|_{T=0} \delta G_c(\omega'). \tag{5.7}$$

In (5.6), we have used δ_T to denote the variation with T which is *not* implicit through $G_c(\omega)$, and G_c^0 is used as a reminder that the variation is calculated with a fixed zero-temperature bath. Equation (5.7) involves the functional derivative of the f self-energy with respect to the bath Green's function. Equations (5.4)–(5.7) can now be substituted into (5.2) to yield

$$\left\{ t^2 + \left[\omega - t^2 G_c(\omega)\right] \left[\omega - 3t^2 G_c(\omega)\right] - \frac{t^2 \langle (T_j^{\text{imp}}(\omega))^2 \rangle^{\text{av}}}{\left[\omega - t^2 G_c(\omega)\right]^2} \right\} \Bigg|_{T=0} \delta G_c(\omega)$$

$$- \int \mathrm{d}\omega' \left. \left\langle \frac{(T_j^{\text{imp}}(\omega))^2}{V_j^2} \frac{\delta \Sigma_{fj}^{\text{imp}}(\omega)}{\delta G_c(\omega')} \right\rangle^{\text{av}} \right|_{T=0} \delta G_c(\omega') = \langle \delta_T T_j^{\text{imp}}(\omega) \rangle^{\text{av}} \Big|_{G_c^0}. \tag{5.8}$$

This is an integral equation for $\delta G_c(\omega)$ whose source term is given by the averaged variation of the T-matrix with the temperature. Without the last term on its left-hand side, equation (5.8) is actually a simple algebraic equation. The last term describes the feedback effect that the change in the self-consistent conduction electron bath generates on the *ensemble* of local impurity actions. Since raising the temperature by a small amount leads to the unquenching of *a few dilute* spins, we do not expect this feedback effect to be large and will thus neglect the last term on the left-hand side of (5.8).

We now analyse the source term on the right-hand side of (5.8). At zero frequency, the imaginary part of the T-matrix can be written as

$$\text{Im}\, T_j^{\text{imp}}(T) = \frac{\sin^2 \delta_{0j}}{\pi \rho_0} t\left(\frac{T}{T_{Kj}}\right) \tag{5.9}$$

where δ_{0j} is the phase shift at $T = 0$. We can write down the asymptotic limits of the scaling function $t(x)$

$$\begin{aligned} t(x) &\approx 1 - \alpha x^2 & (x \ll 1) \\ t(x) &\approx \frac{\beta}{(\ln(x))^2} & (x \gg 1) \end{aligned} \tag{5.10}$$

where α and β are universal numbers. Therefore,

$$\delta_T \,\text{Im}\, T_j^{\text{imp}}(T) = -\frac{\sin^2 \delta_{0j}}{\pi \rho_0} \left[1 - t\left(\frac{T}{T_{Kj}}\right)\right] \equiv -\frac{\sin^2 \delta_{0j}}{\pi \rho_0} F(T/T_{Kj}) \tag{5.11}$$

which defines the function $F(x)$. This function will be averaged over with the distribution
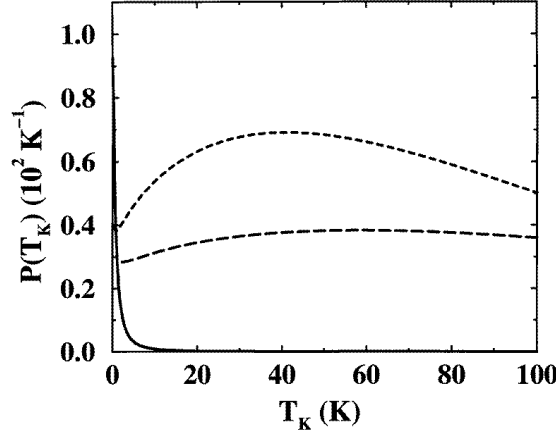
Figure 12. The experimentally determined distribution of Kondo temperatures of the alloys UCu$_{5-x}$Pd$_x$ with $x = 1$ (— — —) and 1.5 (– – –) (from reference [30]) and the function $F(T_K, T)$ (——) defined in the text. The upturn at very low T_Ks is not shown. The function $F(T_K, T)$ only probes the $T_K = 0$ value of the distributions at low T.

of Kondo temperatures. Therefore, *keeping T fixed and as as function of T_K*

$$F(T/T_{Kj}) \approx \frac{\alpha T^2}{T_{Kj}^2} \qquad\qquad (T_{Kj} \gg T)$$

$$F(T/T_{Kj}) \approx 1 - \frac{\beta}{(\ln(T/T_{Kj}))^2} \qquad (T_{Kj} \ll T).$$

(5.12)

It can be seen that $F(T/T_{Kj})$ has a peak at $T_{Kj} = 0$ with width T, decaying rapidly to zero as $1/T_{Kj}^2$ for large T_{Kj} (figure 12). For low temperatures compared with the typical scale of the distribution function $P(T_K)$ one can write

$$\delta_T \operatorname{Im} T_{\text{imp}} \approx -\frac{a \sin^2 \delta_{0j}}{\pi \rho_0} T \delta(T_{Kj})$$

(5.13)

where $a = \int \mathrm{d}x\, F(1/x)$. A similar analysis can be carried out for the real part of the T-matrix. Therefore, after averaging over T_K one gets

$$\langle \delta_T \operatorname{Im} T_j^{\text{imp}}(\omega) \rangle^{\text{av}} \approx -\frac{a P_0 \sin^2 \delta_0}{\pi \rho_0} T$$

(5.14)

consistent with figure 11. It is clear that, as long as the distribution of Kondo temperatures has finite weight at $T_K = 0$, the average T-matrix will show a linear temperature dependence. If $P(0) = 0$ or negligible, then Fermi-liquid behaviour is recovered, with the characteristic T^2-law. The result of (5.14) should be plugged into (5.8) and then into (5.1) for the final expression of the conduction electron self-energy.

As our analysis above has shown, the same physical mechanism underlies the anomalous non-Fermi-liquid behaviour of the resistivity as in the case of the thermodynamic properties. It is the presence of low-T_K spins, unquenched even at low temperatures, which gives rise to anomalous scattering. Though the zero-temperature transport is a reflection of the full structure of the distribution function, the leading low-temperature behaviour is much simpler, corresponding to the gradual decrease of the number of effective scattering centres. Since the number of released spins is small at low temperatures, their effect is additive and an

average over their subtracted T-matrices is well justified. Finally, we add that an immediate consequence of the physical origin of the anomalous scattering in this disorder model is a *negative* magnetoresistance at low temperatures. Much like the temperature, a magnetic field acts to destroy the low-T_K Kondo singlets and thus to suppress their effectiveness as sources of disorder.

6. The dynamic susceptibility

The dynamic susceptibility of $UCu_{5-x}Pd_x$ ($x = 1$ and $x = 1.5$) has been measured with inelastic neutron scattering and reported in reference [33]. The first important result was that the q-dependence of the magnetic response could be completely accounted for by the q-dependence of the uranium-ion form factor, suggesting that the spin dynamics is completely local. Furthermore, as expected, the frequency and temperature dependences of the imaginary part of the dynamic susceptibility are anomalous. There was no significant difference between the magnetic behaviours of the $x = 1$ and the $x = 1.5$ alloys. These results provide a useful testing ground for the disorder model. Indeed, one can use the distribution of Kondo temperatures deduced from the fits to the thermodynamic data to determine the dynamic response and compare with the experimental data. Like the static magnetic susceptibility, the dynamic response will be dominated by a few unquenched spins. Therefore, it is a reasonable assumption to take the overall dynamic lattice response to be essentially given by an average over the single-impurity results. Moreover, the local nature of the measured dynamic susceptibility is consistent with this assumption.

There is currently no complete description of the dynamic susceptibility of a single Kondo impurity for the full range of temperatures and frequencies, though the methods to carry out this task certainly are available. Among the existing results, we cite the unpublished work of Costi and Hewson for the dynamic susceptibility of the Anderson model, quoted in reference [45]. Besides, the non-crossing approximation (NCA) and an extension of it have also been used to determine this response [46]. Quite often, the dynamic susceptibility of a Kondo impurity is fitted to a relaxational form [47]

$$\chi''(\omega, T) = \frac{\chi(T)\Gamma(T)\omega}{\omega^2 + \Gamma^2(T)} \tag{6.1}$$

where $\chi(T)$ is the impurity spin susceptibility and the linewidth $\Gamma(T)$ is a function of temperature only. Note that this form automatically satisfies the Kramers–Kronig relation

$$\chi(T) = \frac{1}{\pi} \int_{-\infty}^{+\infty} \frac{\chi''(\omega, T)}{\omega} \, d\omega. \tag{6.2}$$

The high-temperature behaviour of $\Gamma(T)$ is given the Korringa law with logarithmic corrections [48]:

$$\Gamma(T) \approx 4\pi(\rho_0 J)^2 T \left[1 - 4(\rho_0 J)\ln T\right]. \tag{6.3}$$

At zero temperature, one can use the so-called Shiba relation to determine $\Gamma(0)$ [49]:

$$\lim_{\omega \to \infty} \frac{\chi''(\omega, 0)}{\pi\omega} = \frac{2\chi^2(0)}{(g\mu_B)^2} \implies \Gamma(0) = \frac{2T_K}{w\pi} \tag{6.4}$$

where $w \approx 0.4107$ is the so-called Wilson number. In the absence of a better description, we have employed a crude approximation that interpolates between these two limits

$$\Gamma(T) = \begin{cases} \dfrac{2T_K}{w\pi} & \text{for } T < T_K \\ 4\pi(\rho_0 J)^2 T + \alpha & \text{for } T > T_K \end{cases} \tag{6.5}$$

where α is such that $\Gamma(T)$ is continuous. We stress the crudeness of the approximation and regard it as a rough description of the actual behaviour.
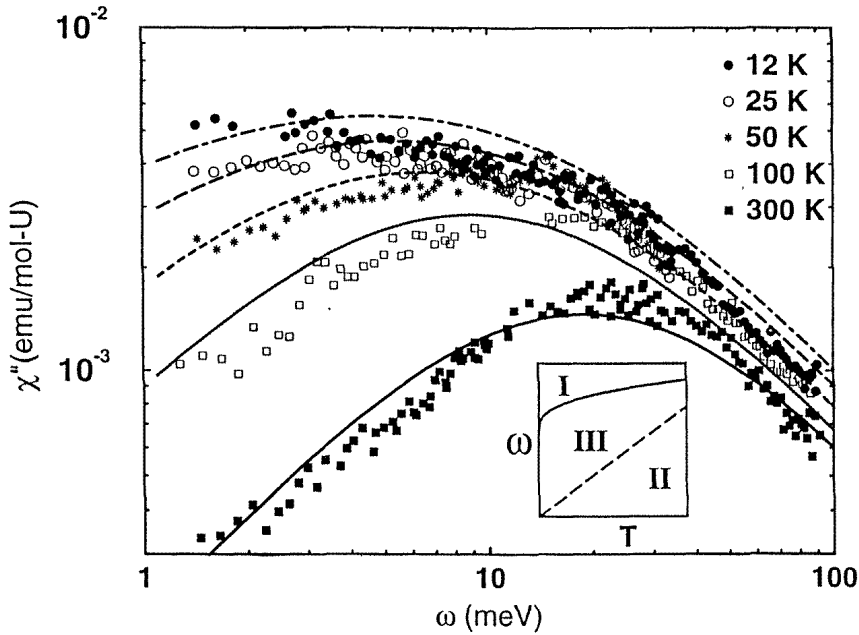

Figure 13. A comparison between the measured dynamic magnetic susceptibility from reference [33] and the prediction of the disorder model. Here, we have used the distribution function appropriate for $x = 3.5$ according to reference [30].

Once the behaviour of the dynamic susceptibility for a Kondo impurity is assumed to be the one given by equations (6.1) and (6.5), one can then easily perform the averaging with the distribution of coupling constants determined experimentally in reference [30]. We have done so and the results are shown in figure 13 ($x = 3.5$) and figure 14 ($x = 4$). We stress that, once the distribution of f-shell parameters is determined from the fits to the static magnetic susceptibility, *no additional fitting is performed.* As can be seen from the figures, the agreement between the experiment and the predictions of the disorder model is rather good, considering the range of frequencies and temperatures and the crudeness of our assumptions. The agreement is slightly better when one uses the distribution of the $x = 3.5$ alloy. Though a more accurate description should be endeavoured, we believe the disorder model cannot be ruled out by the neutron scattering data.

7. Discussion and conclusions

We would like to now pause and consider the overall picture that emerges from the disorder model as well as the drawbacks of our current treatment of the problem. We have emphasized throughout that the important ingredient at the base of all the non-Fermi-liquid features in this approach is the presence of f sites with arbitrarily low local Kondo temperatures. More precisely, $P(T_K = 0) \neq 0$. As the temperature is raised, these low-T_K spins are gradually unquenched and it is this very release process that gives rise to the
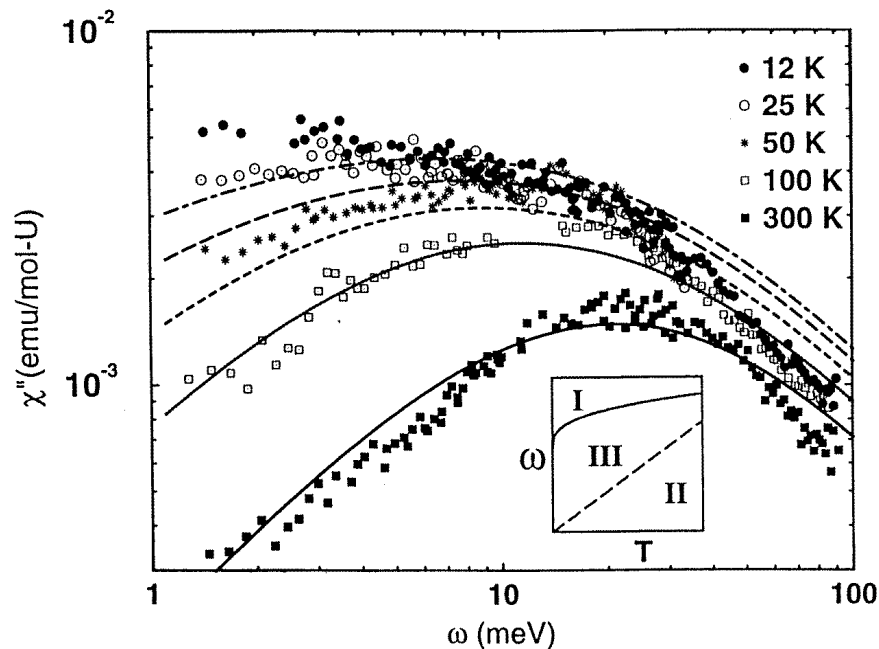
Figure 14. A comparison between the measured dynamic magnetic susceptibility from reference [33] and the prediction of the disorder model. Here, we have used the distribution function appropriate for $x = 4$ according to reference [30].

anomalous thermodynamic as well as transport properties.

One of the practical difficulties that one faces in applying the dynamical field theory is the fact that, due to the very nature of the physics involved, one needs to be able to solve the *ensemble* of impurity models over the whole range of temperatures from $T \ll T_{Kj}$ to $T \gg T_{Kj}$. This is a notoriously difficult task as is evident from the long history that led to the final solution of the Kondo problem. The conventional approach of Wilson's numerical renormalization group, as it is currently formulated, relies on a special 'energy-shell' decimation procedure, which is not obviously adapted to the present case of a general conduction electron density of states. Therefore, in the non-trivial case of the resistivity, we are not yet able to reliably predict the value of the coefficient of the linear term, which might be checked against experiments.

The dynamical mean-field theory does not take into account the RKKY interaction between f sites. These have been studied most extensively in the context of the two-impurity Kondo problem [50]. From these studies it is known that, if the RKKY scale is large enough compared to T_K, the two impurity spins develop strong correlations which tend to lock them into a singlet state, whereby the Kondo effect is killed. Since we rely on the presence of certain sites with very low Kondo temperatures, one might wonder whether the inclusion of RKKY interactions would not effectively provide a low-energy cut-off below which $P(T_K)$ would be essentially negligible. Although we cannot give a rigorous answer to this question, some very general arguments indicate that the possibility of having low-T_K spins is more robust than one might expect.

We have already emphasized that, if the distribution function $P(T_K)$ is broad enough, at low temperatures compared to its overall width, the fraction of spins which remain

unquenched is rather small. Therefore, in general, they form a *dilute* system of spins of density n_{low}, the average distance between them being proportional to $(n_{low})^{-1/3}$. Since the average distance will be large, this will render the RKKY interaction less effective, since its strength decays as R^{-3}. Furthermore, we will argue that the effectiveness of the RKKY interaction in suppressing the Kondo effect is actually a higher-order effect in the dilution n_{low}.

Indeed, consider two low-T_K spins chosen at random in the sample. In general, as argued above, they will be far apart. Now, unlike the usual two-impurity Kondo problem, these two spins will have *different* coupling constants J_1 and J_2 and, therefore, two different Kondo scales T_{K1} and T_{K2}. The RKKY scale $T_{RKKY} \propto J_1 J_2/D$, apart from the dependence on the distance between the spins. Now, in the conventional two-impurity Kondo problem, where $T_{K1} = T_{K2}$, one has, qualitatively, two independent Kondo screening processes, one at each spin, when $T_{K1} = T_{K2} \gg T_{RKKY}$, whereas the effect will be suppressed when $T_{K1} = T_{K2} \ll T_{RKKY}$. In our disordered case, RKKY interaction dominates if, say, $T_{K1} < T_{K2} \ll T_{RKKY}$. However, in the intermediate case when $T_{K1} \ll T_{RKKY} \ll T_{K2}$, two independent Kondo effects will survive, even though T_{RKKY} is still larger than one of the Kondo temperatures. Indeed, as one comes down in energy scale, by the time one hits T_{RKKY}, spin 2 has already undergone quenching and is no longer available to correlate into a singlet-like composite with spin 1. Therefore, the RKKY effectiveness depends on the random selection of two spins, both of which must have low enough Kondo temperatures. We would thus expect it to be of order n_{low}^2. Naturally, the transitions between different regimes are all crossovers (in the absence of special unphysical symmetries) and there will be no sharp distinctions between the different cases and hence no sharp cut-off to the distribution function $P(T_K)$.

We have emphasized throughout our analysis the importance of the structure of the distribution of Kondo temperatures, in particular, whether it has an intercept with the vertical axis at $T_K = 0$ or not. Due to the exponential dependence of T_K on the f parameters, very small modifications in the width of the bare distribution lead to rather large changes in the distribution of Kondo temperatures. If the bare width is too small, $P(T_K)$ will be negligible at low T_K, whereas, if it is too large, $P(T_K)$ will be divergent. Therefore, the situation where $P(T_K)$ can be taken as approximately constant when $T_K \rightarrow 0$ only holds in a narrow window of bare disorder widths, in our current approach. In a more speculative vein, one is tempted to think that the RKKY interaction, which is left out of the current approach, might intervene to impose an upper bound on the density of low-T_K spins which are allowed to exist in such a state. It would do so by effectively eliminating them through the formation of random singlets [27].

Finally, by treating the disorder seen by the conduction electrons in a mean-field CPA-like fashion, we have neglected the effects of fluctuations in the conduction electron density of states. It is natural to expect that these effects might act to further renormalize the distribution of Kondo temperatures. It would be interesting to study whether, like in many other treatments of disordered systems [27], these effects lead to a flow towards a universal form of the distribution function.

In conclusion, we have presented a complete picture of the possible origin of the non-Fermi-liquid behaviour in Kondo alloys. Our study has shown the important effect that correlations have on the role of disorder in f-electron systems, considerably enhancing the bare f-shell disorder strength. The interplay between disorder and correlations leads to the idea of a distribution of Kondo temperatures, whose structure determines whether a Fermi-liquid description is possible. In the particular case when $P(0) \neq 0$, both thermodynamic and transport properties are anomalous and incompatible with a Fermi-liquid picture.

Acknowledgments

Appendix A. A simplified expression for the conductivity

In the case of a semicircular density of states, a simplification of the expression (3.11) can be achieved. Indeed [38],

$$
I = \int d\epsilon \; \rho_0(\epsilon) A^2(\epsilon, \omega) = \int d\epsilon \; \rho_0(\epsilon) \frac{1}{2} \operatorname{Re}\left[G_c(\epsilon, \omega) G_c^*(\epsilon, \omega) - G_c^2(\epsilon, \omega)\right]
$$
$$
= \frac{1}{2}\left\{\operatorname{Re}\left[\frac{\partial G_l(z)}{\partial z}\right] - \frac{\operatorname{Im} G_l(z)}{\operatorname{Im} z}\right\} \tag{A.1}
$$

where $z \equiv \omega + \mu - \Sigma_c(\omega)$ and

$$
G_l(z) \equiv \int d\epsilon \; \frac{\rho_0(\epsilon)}{z - \epsilon}. \tag{A.2}
$$

Using the identity $z = G_l^{-1}(z) + t^2 G_l(z)$, which follows from (3.8), we get

$$
\sigma_{DC} = \frac{2e^2}{\hbar \pi a} \int_{-\infty}^{+\infty} d\omega \left(-\frac{\partial f}{\partial \omega}\right)\left\{\operatorname{Re}\left[\frac{1}{(t^2 G_l(z))^2 - 1}\right] + \frac{1}{1 - |t^2 G_l(z)|^2}\right\}. \tag{A.3}
$$

Appendix B. The conduction electron self-energy and the impurity model T-matrix

The expression for the conduction electron self-energy $\Sigma_c(\omega)$ can be recast in a more illuminating form by employing the T-matrix associated with the impurity problem, which is defined by

$$
T_j^{\mathrm{imp}}(\omega) \equiv V_j^2 G_{fj}^{\mathrm{imp}}(\omega). \tag{B.1}
$$

Inserting this definition into (3.6), then into (3.5) and (3.4), we can write after some manipulations

$$
\overline{G}_c(\omega) = \frac{1}{\omega + \mu - t^2 \overline{G}_c(\omega)} + \frac{\langle T_j^{\mathrm{imp}}(\omega)\rangle^{\mathrm{av}}}{(\omega + \mu - t^2 \overline{G}_c(\omega))^2}. \tag{B.2}
$$

Now, equation (3.8) can be explicitly solved for a semicircular density of states giving

$$
\Sigma_c(\omega) = \omega + \mu - \frac{1}{\overline{G}_c(\omega)} - t^2 \overline{G}_c(\omega). \tag{B.3}
$$

Combining (B.2) and (B.3) we finally get

$$
\Sigma_c(\omega) = \frac{\langle T_j^{\mathrm{imp}}(\omega)\rangle^{\mathrm{av}}}{\overline{G}_c(\omega)(\omega + \mu - t^2 \overline{G}_c(\omega))}. \tag{B.4}
$$

Appendix C. Thermodynamic properties

In this appendix, we will investigate whether the assumptions of the simple disorder model of reference [30] (hereafter, the SDM) are justified within the framework of the dynamical mean-field theory. Let us recapitulate what the assumptions of the SDM are. Essentially, the model assumes a collection of independent Anderson or Kondo impurities, each of which hybridizes with the same, featureless conduction bath. The parameters of this collection of impurities are distributed according to some assumed distribution function(s). In the particular case of reference [30], which assumed Kondo spins, the dimensionless Kondo coupling constant $\lambda \equiv \rho_0 J$ was assumed to be distributed according to a Gaussian. Thermodynamic properties are then calculated by taking the average over the single-impurity results with the appropriate distribution functions, as if the impurity responses were completely uncorrelated.

It is clear that the dynamical mean-field theory retains much of the flavour of the SDM, with the *ensemble* of impurity problems playing the role of the uncorrelated collection of spins. The question that we would like to answer is that of whether the equivalence can be shown within the framework of the dynamical mean-field theory and, more importantly, what are the conditions for the validity of the equivalence. We will confine our analysis to the total energy, which is enough for the calculation of specific heat. The same conclusions apply to the susceptibility, which, however, requires consideration of the free energy.

Let us first write down the total energy in the framework of the dynamical mean-field theory. We have

$$
E_{DMF} = \langle H \rangle = \sum_{ij\sigma} -t_{ij}(\langle c_{i\sigma}^{\dagger} c_{j\sigma} \rangle + \text{HC}) + \sum_{j\sigma} E_j^f \langle f_{j\sigma}^{\dagger} f_{j\sigma} \rangle
$$
$$
+ \sum_{j\sigma} V_j(\langle c_{j\sigma}^{\dagger} f_{j\sigma} \rangle + \text{HC}) + U \sum_j \langle n_{fj\uparrow} n_{fj\downarrow} \rangle. \tag{C.1}
$$

We can write

$$
\langle c_{i\sigma}^{\dagger} c_{j\sigma} \rangle = T \sum_{i\omega_n} G_{c\sigma}^{ij}(i\omega_n). \tag{C.2}
$$

Now, when the coordination number z goes to infinity and for the case of a Bethe lattice (in the absence of symmetry breaking) one can prove that [41]

$$
G_{c\sigma}^{ij}(i\omega_n) = -t_{ij} G_c^2(i\omega_n) \tag{C.3}
$$

from which it follows that

$$
\sum_{ij\sigma} -t_{ij}(\langle c_{i\sigma}^{\dagger} c_{j\sigma} \rangle + \text{HC}) = 2T \sum_{i\omega_n} \sum_{ij} t_{ij}^2 G_c^2(i\omega_n) = 2\mathcal{N} T t^2 \sum_{i\omega_n} \overline{G}_c^2(i\omega_n) \tag{C.4}
$$

where $\mathcal{N}$ is the number of lattice sites and, consistent with the correct rescaling of the hopping in the infinite-coordination limit, $t^2 \equiv z t_{ij}^2$. Plugging (C.4) into (C.1), one then has the total energy completely expressed in terms of local quantities. This is the quantity that we want to compare with the prediction of the SDM.

In order to do that, one needs to define what precisely one means by the SDM. In the dynamical mean-field theory, we have the *ensemble* of impurity models defined by (3.2). We, therefore, *define* the total energy in the SDM by the sum of the energies of the various impurities:

$$
E_{SDM} = \sum_j E^{\text{imp}}\{E_j^f, V_j\}. \tag{C.5}
$$

To define the energy of one impurity, we first write the Hamiltonian corresponding to (3.2):

$$H^{\mathrm{imp}}\left\{E^f, V\right\} = \sum_{k\sigma} E_k a_{k\sigma}^\dagger a_{k\sigma} + \sum_\sigma E^f f_\sigma^\dagger f_\sigma + V \sum_{k\sigma} (a_{k\sigma}^\dagger f_\sigma + \mathrm{HC}) + U \sum_j n_{f\uparrow} n_{f\downarrow}$$

(C.6)

where we introduced fictitious fermionic operators $a_{k\sigma}$ to mimic the self-consistent conduction electron bath through the 'cavity' Green's function of (3.3),

$$\Delta(\omega) \equiv \sum_k \frac{1}{\omega - E_k}.$$

(C.7)

We then define the appropriate single-impurity energy by

$$E^{\mathrm{imp}}\{E_j^f, V_j\} \equiv \left\langle H^{\mathrm{imp}}\left\{E^f, V\right\}\right\rangle - \sum_{k\sigma} E_k \langle a_{k\sigma}^\dagger a_{k\sigma}\rangle\Big|_{V=0}$$

(C.8)

where we subtracted the total energy of the fictitious conduction electron bath evaluated at $V = 0$. Now, the fictitious conduction electron Green's function is

$$G_a(k, k', \omega) = \delta_{kk'} G_a^0(k, \omega) + G_a^0(k, \omega) V^2 G^f(\omega) G_a^0(k', \omega).$$

(C.9)

Using

$$\langle a_{k\sigma}^\dagger a_{k\sigma}\rangle = T \sum_{\mathrm{i}\omega_n} G_a(k, k, \mathrm{i}\omega_n)$$

(C.10)

we have

$$\langle a_{k\sigma}^\dagger a_{k\sigma}\rangle - \langle a_{k\sigma}^\dagger a_{k\sigma}\rangle\Big|_{V=0} = TV^2 \sum_{\mathrm{i}\omega_n} G^f(\mathrm{i}\omega_n) \left[G_a^0(k, \mathrm{i}\omega_n)\right]^2.$$

(C.11)

Thus

$$\sum_{k\sigma} E_k \left[\langle a_{k\sigma}^\dagger a_{k\sigma}\rangle - \langle a_{k\sigma}^\dagger a_{k\sigma}\rangle\Big|_{V=0}\right] = 2TV^2 \sum_{\mathrm{i}\omega_n} G^f(\mathrm{i}\omega_n) \sum_k \frac{E_k}{(\mathrm{i}\omega_n - E_k)^2}$$

$$= -2TV^2 \sum_{\mathrm{i}\omega_n} G^f(\mathrm{i}\omega_n) \left[\Delta(\mathrm{i}\omega_n) + \mathrm{i}\omega_n \frac{\partial \Delta(\mathrm{i}\omega_n)}{\partial(\mathrm{i}\omega_n)}\right].$$

(C.12)

In the last equality we used (C.7).

We can now use equations (C.1), (C.5), (C.6) and (C.8) to write the difference in energy between the SDM and the dynamical mean-field theory:

$$\Delta E \equiv E_{DMF} - E_{SDM} = \sum_{k\sigma} \left\{E_k \left[\langle a_{k\sigma}^\dagger a_{k\sigma}\rangle\Big|_{V=0} - \langle a_{k\sigma}^\dagger a_{k\sigma}\rangle\right] + (\epsilon_k - \mu)\langle c_{k\sigma}^\dagger c_{k\sigma}\rangle\right\}.$$

(C.13)

To simplify things further, we can use equations (C.4) and (C.12) to get

$$\Delta E = 2T \sum_{\mathrm{i}\omega_n} \left\{\mathcal{N} t^2 \overline{G}_c^2(\mathrm{i}\omega_n) + \sum_j V_j^2 G_j^f(\mathrm{i}\omega_n)\left[\Delta(\mathrm{i}\omega_n) + \mathrm{i}\omega_n \frac{\partial \Delta(\mathrm{i}\omega_n)}{\partial(\mathrm{i}\omega_n)}\right]\right\}.$$

(C.14)

We then use (B.2) and the definition (3.3) to arrive at our final expression for the difference in energy between the dynamical mean-field theory and the SDM:

$$\frac{\Delta E}{\mathcal{N}} = 2T \sum_{\mathrm{i}\omega_n} \left\{t^2 \overline{G}_c^2(\mathrm{i}\omega_n) + \left[\frac{\overline{G}_c(\mathrm{i}\omega_n)}{\Delta(\mathrm{i}\omega_n)} - 1\right]\left[1 + \frac{\partial \ln \Delta(\mathrm{i}\omega_n)}{\partial \ln(\mathrm{i}\omega_n)}\right]\right\}.$$

(C.15)

We are now in a position to determine whether the SDM is accurate enough to give the thermodynamic properties of the system within the dynamical mean-field-theory framework.

For this, it is enough to consider (C.13). All of the quantities in this equation are related to conduction electron kinetic properties. The corresponding densities of states are given by the imaginary parts of either $\overline{G}_c(\omega)$ or the 'cavity' Green's function $\Delta(\omega)$. As can be clearly seen from figures 3 and 4, these quantities are weakly renormalized. Their contributions to, say, the specific heat coefficient $\gamma = C_V(T)/T$ are of the order of $1/D$ and are completely negligible when compared to the contribution from the impurity part, which is of order $1/T_K \gg 1/D$. Therefore, as far as thermodynamic properties such as γ and χ are concerned, the approximation of averaging over single-impurity results is perfectly consistent with the solution of the full dynamical mean-field theory. This is true of both the clean and the dirty systems, since nothing in this argument relied on the presence of disorder. However, we stress the fact that the *ensemble* of impurity problems must be solved in the *fully self-consistent conduction electron bath*. Though the renormalizations of this bath are small, they affect the impurity properties through the conduction electron density of states ρ_0. The latter quantity appears in the argument of the exponential in the expression for the Kondo temperature and can, therefore, lead to rather substantial renormalizations of the total energy. To fully describe these changes, one needs to solve the full dynamical mean-field theory equations.

Appendix D. The slave-boson mean-field theory of the impurity models

The slave-boson description of the infinite-U Anderson model starts with the replacement of the non-holonomic constraint $n_f < 1$ imposed by the $U \to \infty$ condition by a new set of slave-boson operators b_j together with a holonomic constraint [35]:

$$f_{j\sigma} \longrightarrow b_j^\dagger f_{j\sigma} \tag{D.1}$$

$$n_{fj\sigma} \longrightarrow n_{fj\sigma} \tag{D.2}$$

$$\sum_\sigma (n_{fj\sigma}) < 1 \longrightarrow \sum_\sigma (n_{fj\sigma}) + b_j^\dagger b_j = 1. \tag{D.3}$$

The constraint is then imposed by introducing a Lagrange multiplier term in the Lagrangian:

$$\mathcal{L}_0 \longrightarrow \mathcal{L}_0 + \mathrm{i} \int_0^\beta \mathrm{d}\tau\, \lambda_j(\tau) \left[\sum_\sigma f_{fj\sigma}^\dagger(\tau) f_{fj\sigma}(\tau) + b_j^\dagger(\tau) b_j(\tau) - 1 \right] \tag{D.4}$$

where $\lambda_j(\tau)$ is an additional bosonic field variable. The transformed action corresponding to the impurity action (3.2) is then

$$S_j^{\mathrm{imp}} = S_{1j}^{\mathrm{imp}} + S_{2j}^{\mathrm{imp}}$$

$$S_{1j}^{\mathrm{imp}} = \int_0^\beta \mathrm{d}\tau \left[\sum_\sigma f_{j\sigma}^\dagger(\tau) \left[\partial_\tau + E_j^f + \mathrm{i}\lambda_j(\tau) \right] f_{j\sigma}(\tau) \right.$$

$$\left. + b_j^\dagger(\tau) \left[\partial_\tau + \mathrm{i}\lambda_j(\tau) \right] b_j(\tau) - \mathrm{i}\lambda_j(\tau) \right]$$

$$S_{2j}^{\mathrm{imp}} = \int_0^\beta \mathrm{d}\tau \int_0^\beta \mathrm{d}\tau' \sum_\sigma f_{j\sigma}^\dagger(\tau) b_j(\tau) V_j^2 \Delta(\tau - \tau') f_{j\sigma}(\tau') b_j^\dagger(\tau') \tag{D.5}$$

where $\Delta(\tau)$ is the Matsubara–Fourier transform of (3.3). Note that the second part of the impurity action, which corresponds to hybridization processes between the f site and the effective conduction electron bath, has been modified by the introduction of the slave-boson field $b_j(\tau)$, which deals with the bookkeeping of the occupation of the f site.

At the mean-field level, the bosonic fields $b_j(\tau)$ and $\lambda_j(\tau)$ acquire a time-independent expectation value and behave as c-numbers [35]. The resulting effective action is quadratic in the pseudo-f electrons and can be exactly solved. Following the convention of writing $i\langle\lambda_j\rangle = \epsilon_j^f - E_j^f$ and $\langle b_j\rangle = r_j$, it reads

$$S_j^{\text{eff}} = T\sum_{\omega_n\sigma}\left[f_{j\sigma}^\dagger(i\omega_n)(-i\omega_n + \epsilon_j^f + r_j^2 V_j^2\Delta(i\omega_n))f_{j\sigma}(i\omega_n)\right] + (\epsilon_j^f - E_j^f)(r_j^2 - 1). \quad \text{(D.6)}$$

The mean-field parameters r_j and ϵ_j^f are determined by a saddle-point extremization of the free energy corresponding to (D.6). The mean-field equations then read

$$\frac{2}{\pi}\int_{-\infty}^{\infty} d\omega\, \frac{f(\omega)\tilde{\Delta}_j''(\omega)}{(\omega - \epsilon_j^f - \tilde{\Delta}_j'(\omega))^2 + (\tilde{\Delta}_j''(\omega))^2} + r_j^2 - 1 = 0 \quad \text{(D.7)}$$

$$\frac{2}{\pi}\int_{-\infty}^{\infty} d\omega\, \frac{f(\omega)\tilde{\Delta}_j''(\omega)(\omega - \epsilon_j^f)}{(\omega - \epsilon_j^f - \tilde{\Delta}_j'(\omega))^2 + (\tilde{\Delta}_j''(\omega))^2} + r_j^2(\epsilon_j^f - E_j^f) = 0 \quad \text{(D.8)}$$

where $f(\omega)$ is the Fermi function, $\tilde{\Delta}_j(\omega) = r_j^2 V_j^2\Delta(\omega)$, and single and double primes denote real and imaginary parts, respectively. We note that, given the hybridization function $\Delta(i\omega_n)$, each value of the bare parameters E_j^f and V_j will define a different impurity problem with its own corresponding values of r_j and ϵ_j^f. Thus, a distribution of mean-field parameters is also generated.

The mean-field treatment that we have described gives the following expression for the f-electron Green's function:

$$G_{fj}(i\omega_n) = \frac{r_j^2}{i\omega_n - \epsilon_j^f - r_j^2 V_j^2\Delta(i\omega_n)}. \quad \text{(D.9)}$$

Note that the numerator in (D.9) is crucial. It is a consequence of the slave-boson prescription (D.1) and distinguishes the pseudo-f-electron Green's function, from which it is absent, from the real-f-electron Green's function. Finally, using the definition (3.6), one can write the mean-field expression for the f-electron self-energy:

$$\Sigma_{fj}(i\omega_n) = i\omega_n - E_j^f - \frac{(i\omega_n - \epsilon_j^f)}{r_j^2} \quad \text{(D.10)}$$

which yields

$$\Phi_j(i\omega_n) = \frac{r_j^2 V_j^2}{i\omega_n - \epsilon_j^f}. \quad \text{(D.11)}$$

This can then be inserted into (3.4), thus closing the self-consistency loop. Note that, in the pure case,

$$\Sigma_c(\omega) = \Phi(\omega) = \frac{r^2 V^2}{\omega - \epsilon_j^f} \quad \text{(D.12)}$$

which is consistent with the low-energy Fermi-liquid parametrization of (4.2).

References

[1] Landau L D 1956 *Sov. Phys.–JETP* **3** 920; 1957 *Sov. Phys.–JETP* **5** 101; 1959 *Sov. Phys.–JETP* **8** 70
[2] Anderson P W 1984 *Basic Notions of Condensed Matter Physics* (Menlo Park, CA: Benjamin/Cummings) ch 3, p 70

[3] Wilson K G 1979 *Rev. Mod. Phys.* **47** 773
[4] Noziéres P 1974 *J. Low Temp. Phys.* **17** 31
   Krishna-murthy H R, Wilkins J W and Wilson K G 1980 *Phys. Rev.* B **21** 1003, 1044
[5] Leggett A J 1965 *Phys. Rev. Lett.* **14** 536; 1965 *Phys. Rev.* A **140** 1869
[6] Migdal A B 1967 *Theory of Finite Fermi Systems and Applications to Atomic Nuclei* (London: Pergamon)
[7] Castellani C, Kotliar G and Lee P A 1987 *Phys. Rev. Lett.* **59** 323
   Castellani C, DiCastro C, Kotliar G, Lee P A and Strinati G 1987 *Phys. Rev. Lett.* **59** 477
[8] For extensive reviews see, e.g.,
   Ginsberg D M 1996 *Physical Properties of High Temperature Superconductors* vols I to V (Singapore: World Scientific)
[9] Maple M B *et al* 1995 *J. Low Temp. Phys.* **99** 223
[10] Maple M B 1996 *J. Phys.: Condens. Matter* **8** 9773
[11] For reviews see, e.g.,
   Lee P A, Rice T M, Serene J W, Sham L J and Wilkins J W 1986 *Comment. Condens. Matter Phys.* **12** 99
   Grewe N and Steglich F 1991 *Handbook on the Physics and Chemistry of Rare Earths* vol 14, ed K A Gschneider and L Eyring (Amsterdam: North-Holland) p 343
[12] von Löhneysen H, Pietrus T, Portisch G, Schlager H G, Schröder A, Sieck M and Trappmann T 1994 *Phys. Rev. Lett.* **72** 3262
   Bogenberger B and von Löhneysen H 1995 *Phys. Rev. Lett.* **74** 1016
[13] Julian S R, Mathur N D, Grosche F M and Lonzarich G G 1996 Non-Fermi liquid to superconducting transition in CePd$_2$Si$_2$ at high pressures *Preprint*
   Grosche F M, Julian S R, Mathur N D and Lonzarich G G 1996 *Physica* B **223+224** 50
[14] Continentino M A 1993 *Phys. Rev.* B **47** 11587
   Millis A J 1993 *Phys. Rev.* B **48** 7183
   Tsvelik A M and Reizer M 1993 *Phys. Rev.* B **48** 9887
[15] Andraka B and Stewart G R 1993 *Phys. Rev.* B **47** 3208
[16] Degiorgi L and Ott H R 1996 *J. Phys.: Condens. Matter* **8** 9901
[17] Seaman C L, Maple M B, Lee B W, Ghamaty S, Torikachvili M S, Kang J-S, Liu L Z, Allen J W and Cox D L 1991 *Phys. Rev. Lett.* **67** 2882
   Andraka B and Tsvelik A M 1991 *Phys. Rev. Lett.* **67** 2886
[18] Degiorgi L, Ott H R and Hulliger F 1995 *Phys. Rev.* B **52** 42
[19] Andraka B 1994 *Phys. Rev.* B **49** 3589
[20] Degiorgi L, Wachter P, Maple M B, de Andrade M C and Herrmann J 1996 *Phys. Rev.* B **54** 6065
[21] Andraka B 1994 *Phys. Rev.* B **49** 348
[22] Amitsuka H and Sakakibara T 1994 *J. Phys. Soc. Japan* **63** 736
   Amitsuka H, Hidano T, Sakakibara T, Suzuki T, Akazawa T and Fujita T 1995 *J. Magn. Magn. Mater.* **140+144** 1403
   Amitsuka H, Shimamoto T, Honma T and Sakakibara T 1995 *Physica* B **206+207** 461
[23] Nozières P and Blandin A 1980 *J. Physique* **41** 193
   Cox D L 1987 *Phys. Rev. Lett.* **59** 1240
   Kim T-S and Cox D L 1995 *Phys. Rev. Lett.* **75** 1622
   Cox D L 1993 *Physica* B **186+188** 312
   Kim T-S and Cox D L 1996 *Phys. Rev.* B **54** 6494
   Kim T-S, Oliveira L N and Cox D L 1996 *Preprint* cond-mat/9606095
[24] Aronson M C, Maple M B, de Sa P, Tsvelik A M and Osborn R 1996 Non-Fermi liquid scaling in the uranium alloys UCu$_{5-x}$Pd$_x$: a phenomenological description *Preprint*
[25] Cox D L 1996 *Physica* B **223+224** 453
   Jarrell M, Pang H, Cox D L and Luk K H 1996 *Phys. Rev. Lett.* **77** 1612
[26] Si Q and Kotliar G 1993 *Phys. Rev. Lett.* **70** 3143; 1993 *Phys. Rev.* B **48** 13 881
   Kotliar G and Si Q 1996 *Phys. Rev.* B **53** 12 373
[27] Bhatt R N and Lee P A 1982 *Phys. Rev. Lett.* **48** 344
[28] Sachdev S 1989 *Phys. Rev.* B **39** 5297
   Milovanović M, Sachdev S and Bhatt R N 1989 *Phys. Rev. Lett.* **63** 82
[29] Bhatt R N and Fisher D S 1992 *Phys. Rev. Lett.* **68** 3072
   Dobrosavljević V, Kirkpatrick T R and Kotliar G 1992 *Phys. Rev. Lett.* **69** 1113
[30] Bernal O O, MacLaughlin D E, Lukefahr H G and Andraka B 1995 *Phys. Rev. Lett.* **75** 2023
   See also
   1996 *J. Phys.: Condens. Matter* **8** (48) (this issue)

[31] Miranda E, Dobrosavljević V and Kotliar G 1996 *Preprint*
[32] Griffiths R B 1969 *Phys. Rev. Lett.* **23** 17
[33] Aronson M C, Osborn R, Robinson R A, Lynn J W, Chau R, Seaman C L and Maple M B 1995 *Phys. Rev. Lett.* **75** 725
    See also
    1996 *J. Phys.: Condens. Matter* **8** (48) (this issue)
[34] Onuki Y, Shimizu Y, Nishihara M, Machii Y and Komatsubara T 1985 *J. Phys. Soc. Japan* **54** 1964
    Onuki Y and Komatsubara T 1987 *J. Magn. Magn. Mater.* **63+64** 281
    Lin C L, Wallash A, Crow J E, Mihalisin T and Schlottmann P 1987 *Phys. Rev. Lett.* **58** 1232
    Kim J S and Stewart G R 1994 *Phys. Rev.* B **49** 327
[35] Coleman P 1983 *Phys. Rev.* B **29** 3035
    Read N and Newns D M 1983 *J. Phys. C: Solid State Phys.* **16** 3273, L1055
    Coleman P 1987 *Phys. Rev.* B **35** 5072
[36] Tešanović Z 1986 *Phys. Rev.* B **34** 5212
[37] Freytag R and Keller J 1990 *Z. Phys.* B **80** 241
    Sollie R and Schlottmann P 1991 *J. Appl. Phys.* **69** 5478; 1991 *J. Appl. Phys.* **70** 5803
    Schlottmann P 1992 *Phys. Rev.* B **46** 998
[38] Wermbter S, Sabel K and Czycholl G 1996 *Phys. Rev.* B **53** 2528
[39] Metzner W and Vollhardt D 1989 *Phys. Rev. Lett.* 62 324
    Georges A and Kotliar G 1992 *Phys. Rev.* B **45** 6479
    Georges A, Kotliar G and Si Q 1992 *Int. J. Mod. Phys.* B **6** 705
    Jarrell M 1995 *Phys. Rev.* B **51** 7429
    Rozenberg M J 1995 *Phys. Rev.* B **52** 7369
[40] Janiš V and Vollhardt D 1992 *Phys. Rev.* B **46** 15 712
    Janiš V, Ulmke M and Vollhardt D 1993 *Europhys. Lett.* **24** 287
    Dobrosavljević V and Kotliar G 1993 *Phys. Rev. Lett.* **71** 3218; 1994 *Phys. Rev.* B **50** 1430
[41] For a recent review of this method see
    Georges A, Kotliar G, Krauth W and Rozenberg M J 1996 *Rev. Mod. Phys.* **68** 13
[42] Khurana A 1990 *Phys. Rev. Lett.* **64** 1990
[43] Economou E N 1983 *Green's Functions in Quantum Physics* (Berlin: Springer) p 141
[44] See, e. g.,
    Hewson A C 1993 *The Kondo Problem to Heavy Fermions* (Cambridge: Cambridge University Press) section 5
[45] Hewson A C 1993 *The Kondo Problem to Heavy Fermions* (Cambridge: Cambridge University Press) pp 286–7
[46] Bickers N E, Cox D L and Wilkins J H 1987 *Phys. Rev.* B **36** 2036
    Anders F B 1995 *J. Phys.: Condens. Matter* **7** 2801
[47] Korringa J 1950 *Physica* **19** 601
[48] Walker M B 1970 *Phys. Rev.* B **1** 3690
[49] Shiba H 1975 *Prog. Theor. Phys.* **54** 967
[50] Jones B A and Varma C M 1987 *Phys. Rev. Lett.* **58** 843
    Jones B A, Varma C M and Wilkins J W 1987 *Phys. Rev. Lett.* **61** 125
    Jones B A and Varma C M 1989 *Phys. Rev.* B **40** 324
    Fye R M and Hirsch J E 1989 *Phys. Rev.* B **40** 4780
    Sakai O, Shimizu Y and Kasuya T 1990 *Solid State Commun.* **75** 81
    Sakai O and Shimizu Y 1992 *J. Phys. Soc. Japan* **61** 2333
    Affleck I and Ludwig A W W 1992 *Phys. Rev. Lett.* **68** 1046
    Affleck I, Ludwig A W W, Pang H-B and Cox D L 1992 *Phys. Rev.* B **45** 7918
    Fye R M 1994 *Phys. Rev. Lett.* **72** 916
    Affleck I, Ludwig A W W and Jones B A 1995 *Phys. Rev.* B **52** 9528